MANCHESTER 1824
The University of Manchester

The University of Manchester Research

Development of West-European PM2.5 and NO2 land use regression models incorporating satellite-derived and chemical transport modelling data

DOI:
10.1016/j.envres.2016.07.005

Document Version
Accepted author manuscript

Link to publication record in Manchester Research Explorer

Citation for published version (APA):
de Hoogh, K., Gulliver, J., van Donkelaar, A., Martin, R. V., Marshall, J. D., Bechle, M. J., Cesaroni, G., Pradas, M. C., Dedele, A., Eeftens, M., Forsberg, B., Galassi, C., Heinrich, J., Hoffmann, B., Jacquemin, B., Katsouyanni, K., Korek, M., Künzli, N., Lindley, S., ... Hoek, G. (2016). Development of West-European PM2.5 and NO2 land use regression models incorporating satellite-derived and chemical transport modelling data. *Environmental Research*, *151*, 1-10. https://doi.org/10.1016/j.envres.2016.07.005

Published in:
Environmental Research

Citing this paper
Please note that where the full-text provided on Manchester Research Explorer is the Author Accepted Manuscript or Proof version this may differ from the final Published version. If citing, it is advised that you check and use the publisher's definitive version.

General rights
Copyright and moral rights for the publications made accessible in the Research Explorer are retained by the authors and/or other copyright owners and it is a condition of accessing publications that users recognise and abide by the legal requirements associated with these rights.

Takedown policy
If you believe that this document breaches copyright please refer to the University of Manchester's Takedown Procedures [http://man.ac.uk/04Y6Bo] or contact openresearch@manchester.ac.uk providing relevant details, so we can investigate your claim.

OPEN ACCESS

Download date:18. May. 2025

Development of West-European $PM_{2.5}$ and NO_2 land use regression models incorporating satellite-derived and chemical transport modelling data

Authors

1. Kees de Hoogh*[1,2]
2. John Gulliver[3]
3. Aaron van Donkelaar[4]
4. Randall V. Martin[4,5]
5. Julian D. Marshall[6]
6. Matthew J. Bechle[6]
7. Giulia Cesaroni [7]
8. Marta Cirach Pradas [8,9]
9. Audrius Dedele[10]
10. Marloes Eeftens[1,2]
11. Bertil Forsberg[11]
12. Claudia Galassi[12]
13. Joachim Heinrich[13,14]
14. Barbara Hoffmann[15,16]
15. Bénédicte Jacquemin[17,18,8,19]
16. Klea Katsouyanni[20,21]
17. Michal Korek[22]
18. Nino Künzli[1,2]
19. Sarah J. Lindley[23]
20. Johanna Lepeule[24]
21. Frederik Meleux[25]
22. Audrey de Nazelle[26]
23. Mark Nieuwenhuijsen[8,9,27]
24. Wenche Nystad[28]
25. Ole Raaschou-Nielsen[29,30]
26. Annette Peters[31]
27. Vincent-Henri Peuch[32]
28. Laurence Rouil[25]
29. Orsolya Udvardy[33]
30. Rémy Slama[24]
31. Morgane Stempfelet[34]
32. Euripides G. Stephanou[35]
33. Ming Y. Tsai[1,2,36]
34. Tarja Yli-Tuomi[37]
35. Gudrun Weinmayr[15, 38]
36. Bert Brunekreef[39,40]
37. Danielle Vienneau[1,2]
38. Gerard Hoek[39]

*Corresponding Author

Kees de Hoogh, Swiss Tropical and Public Health Institute, Socinstrasse 57, 4051 Basel, Switzerland, tel: +41 (0)61 284 8749, Fax +41 61 284 81 01, c.dehoogh@unibas.ch

1. Swiss Tropical and Public Health Institute, Socinstrasse 57, 4051 Basel, Switzerland.
2. University of Basel, Petersplatz 1, 4001 Basel, Switzerland.
3. MRC-PHE Centre for Environment and Health, Department of Epidemiology and Biostatistics, Imperial College London, St Mary's Campus, Norfolk Place, W2 1PG, London, United Kingdom.
4. Department of Physics and Atmospheric Science, Dalhousie University, 6310 Coburg Rd., Halifax, NS B3H 4R2, Canada
5. Harvard-Smithsonian Center for Astrophysics, 60 Garden Street, Cambridge, Massachusetts, MA 02138, USA
6. John R. Kiely Professor of Civil & Environmental Engineering,University of Washington, Wilcox 268, Seattle WA 98195, USA
7. Department of Epidemiology, Lazio Regional Health Service, Via Cristoforo Colombo, 112 - 00147 Rome, Italy
8. Centre for Research in Environmental Epidemiology (CREAL), Doctor Aiguader 88, E-08003 Barcelona, Spain;
9. CIBER Epidemiología y Salud Pública (CIBERESP), Av. Monforte de Lemos, 3-5. Pabellón 11. Planta 0 28029 Madrid, Spain
10. Department of Environmental Sciences, Vytauto Didziojo Universitetas, K. Donelaicio 58, Kaunas 44248, Lithuania
11. Department of Public Health and Clinical Medicine, Occupational and Environmental Medicine, Umea University, SE-901 87 Umea, Sweden.
12. Unit of Cancer Epidemiology, Citta' della Salute e della Scienza University Hospital and Centre for Cancer Prevention, Corso Bramante, 88, 10126 Turin, Italy
13. Ludwig Maximilians University Munich University Hospital Munich Institute and Outpatient Clinic for Occupational, Social and Environmental Medicine Ziemssenstr. 1 D-80336 Munich, Germany
14. Helmholtz Zentrum München - German Research Center for Environmental Health, Institute of Epidemiology I, Ingolstädter Landstr. 1,D-85764 Neuherberg, Germany
15. IUF Leibniz Research Institute for Environmental Medicine, University of Düsseldorf, Auf'm Hennekamp 50, 40225 Düsseldorf, Germany
16. Medical Faculty, Heinrich-Heine University of Düsseldorf, Universitätsstr. 1, 40225 Düsseldorf, Germany
17. INSERM, U1168, VIMA: Aging and chronic diseases. Epidemiological and public health approaches, 16, avenue Paul Vaillant Couturier, 94807, Villejuif, France
18. Université Versailles St-Quentin-en-Yvelines, UMR-S 1168, 2 Avenue de la Source de la Bièvre – 78180, Montigny le Bretonneux, France
19. Universitat Pompeu Fabra (UPF), Plaça de la Mercè, 10-12. 08002, Barcelona, Spain
20. Department of Hygiene, Epidemiology and Medical Statistics, University of Athens Medical School 75, Mikras Asias street 115 27 Athens, Greece
21. Department of Primary Care & Public Health Sciences and Environmental Research Group, King's College London, Franklin-Wilkins Building, 150 Stamford Street, London SE1 9NH
22. Institute of Environmental Medicine, Karolinska Institutet, Nobels väg 13, 171 65 Solna, Stockholm, Sweden
23. Geography, School of Environment, Education and Development, University of Manchester, Manchester M13 3PL, UK

24. Inserm and Univ. Grenoble-Alpes, IAB (U1209), Team of Environmental Epidemiology, 38000 Grenoble, France.
25. National Institute for industrial Environment and Risks (INERIS), Parc Technologique ALATA, 60550 Verneuil en Halatte, France
26. Centre for Environmental Policy, Imperial College London, South Kensington Campus, London SW7 2AZ, UK.
27. IMIM (Hospital del Mar Research Institute), Dr. Aiguader, 88, 08003, Barcelona, Spain
28. Division of Environmental Medicine, Norwegian Institute of Public Health, PO Box 4404 Nydalen, N-0403, Oslo, Norway
29. Danish Cancer Society Research Center, Strandboulevarden 49, DK-2100, Copenhagen, Denmark
30. Department of Environmental Science, Aarhus University, Frederiksborgvej 399, P.O. Box 358, DK-4000, Roskilde, Denmark
31. Institute of Epidemiology II, Helmholtz Zentrum München, German Research Center for Environmental Health, Ingolstädter Landstr. 1, D-85764, Neuherberg, Germany
32. ECMWF, Shinfield Park, Reading, RG2 9AX United Kingdom
33. National Public Health Center, Albert Flórián út 2-6, H-1097 Budapest, Hungary
34. French Institut for Public Health, 12, rue du Val d'Osne, 94415, Saint-Maurice, France
35. Environmental Chemical Processes Laboratory (ECPL), Department of Chemistry, University of Crete, 71003 Heraklion, Greece
36. Department of Environmental and Occupational Health Sciences, University of Washington, Box 357234, Seattle, WA 98195, USA
37. National Institute for Health and Welfare (THL), Department of Health Protection, Living Environment and Health Unit, P.O. Box 95, FI-70701, Kuopio, Finland
38. Institute of Epidemiology and Medical Biometry, Ulm University, Helmholtzstr. 22, 89081, Ulm, Germany
39. Institute for Risk Assessment Sciences, Utrecht University, Yalelaan 2, 3584 CM, Utrecht, The Netherlands.
40. Julius Center for Health Sciences and Primary Care, University Medical Center Utrecht, Universiteitsweg 100, 3584 CG, Utrecht, The Netherlands

Email addresses:

1. c.dehoogh@unibas.ch, 2. j.gulliver@imperial.ac.uk, 3. kelaar@Dal.Ca, 4. Randall.Martin@Dal.Ca, 5, julian@umn.edu, 6. bechl002@umn.edu, 7. g.cesaroni@deplazio.it, 8. mcirach@creal.cat, 9. a.dedele@gmf.vdu.lt, 10. Marloes.eeftens@unibas.ch, 11. bertil.forsberg@envmed.umu.se, 12. claudia.galassi@cpo.it, 13. heinrich@helmholtz-muenchen.de, 14. Barbara.Hoffmann@IUF-Duesseldorf.de, 15. benedicte.jacquemin@inserm.fr, 16. kkatsouy@med.uoa.gr, 17. Michal.Korek@ki.se, 18. Nino.kuenzli@unibas.ch, 19. sarah.lindley@manchester.ac.uk, 20. johanna.lepeule@ujf-grenoble.fr, 21. Frederik.MELEUX@ineris.fr, 22. anazelle@imperial.ac.uk, 23. mnieuwenhuijsen@creal.cat, 24 Wenche.Nystad@fhi.no, 25. ole@cancer.dk, 26. peters@helmholtz-muenchen.de, 27. Vincent-Henri.Peuch@ecmwf.int, 28, Laurence.ROUIL@ineris.fr, 29. udvardy.orsolya@oki.antsz.hu, 30. remy.slama@ujf-grenoble.fr, 31. m.stempfelet@invs.sante.fr, 32. Euripides.Stephanou@gmail.com, 33. m.tsai@unibas.ch, 34. tarja.yli-tuomi@thl.fi, 35. gudrun.weinmayr@uni-ulm.de, 36. B.Brunekreef@uu.nl, 37. Danielle.vienneau@unibas.ch, 38. G.Hoek@uu.nl

Acknowledgements/Funding

The research was supported by funding from the European Community's Seventh Framework Program EXPOsOMICS and ESCAPE studies under grant agreement numbers: FP7 308610 and FP7 211250 respectively. The Air quality modelling data were produced within MACC projects funded by the European Commission under the EU Seventh Research Framework Programme (grant agreement no. 283576, MACC II).

This study does not involve human subjects.

Abstract

Satellite-derived (SAT) and chemical transport model (CTM) estimates of $PM_{2.5}$ and NO_2 are increasingly used in combination with Land Use Regression (LUR) models. We aimed to compare the contribution of SAT and CTM data to the performance of LUR $PM_{2.5}$ and NO_2 models for Europe.

Four sets of models, all including local traffic and land use variables, were compared (LUR without SAT or CTM, with SAT only, with CTM only, and with both SAT and CTM). LUR models were developed using two monitoring data sets: $PM_{2.5}$ and NO_2 ground level measurements from the European Study of Cohorts for Air Pollution Effects (ESCAPE) and from the European AIRBASE network.

LUR $PM_{2.5}$ models including SAT and SAT+CTM explained ~60% of spatial variation in measured $PM_{2.5}$ concentrations, substantially more than the LUR model without SAT and CTM (adjR^2: 0.33-0.38). For NO_2 CTM improved prediction modestly (adjR^2: 0.58) compared to models without SAT and CTM (adjR^2: 0.47-0.51). Both monitoring networks are capable of producing models explaining the spatial variance over a large study area.

SAT and CTM estimates of $PM_{2.5}$ and NO_2 significantly improved the performance of high spatial resolution LUR models at the European scale for use in large epidemiological studies.

Keywords

Air pollution, Exposure, Spatial modelling, Fine particulate matter, Nitrogen dioxide

Graphical Abstract

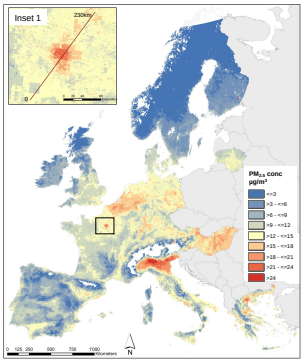

Highlights

- Satellite and chemical transport model data enhanced LUR exposure models.
- This is the first detailed $PM_{2.5}$ surface for Western Europe.
- Routine and purpose-designed air monitoring are comparable for exposure modelling.
- These 100m annual mean $PM_{2.5}$ and NO_2 estimates will be made freely available.

Abbreviations

AB - absolute bias

AE - absolute error

AIRBASE – European air quality database

AOD - aerosol optical depth

COHOV – cross-over-hold-out-validation

COV - cross-over-validation

CTM – Chemical Transport Model

ESCAPE - European Study of Cohorts for Air Pollution Effects

FB - fractional bias

HOV – hold-out-validation

LUR – Land Use Regression

MB - mean bias

ME - mean error

SAT – Satellite-derived

1. Introduction

Recent studies have indicated that long-term air pollution concentrations can have adverse health effects even below current air quality standards.[1,2] To further quantify effects on health outcomes at these lower air pollution levels, it is necessary to undertake large epidemiological studies and/or pool data from multiple cohorts. Air pollution exposure estimates over large geographic areas at sufficient fine spatial resolution are thus needed.

Land use regression (LUR) models have been used extensively in the past decade to assess air pollution exposure at a fine spatial scale for epidemiological studies.[1,2] Most of the applications of LUR models in epidemiology involve relatively small study areas. For application to large areas, such as continents, modelling the background concentration is a challenge for LUR models as LUR cannot explicitly model secondary formation of components and losses due to deposition and other processes.

To improve prediction of background ground level concentrations, satellite-derived data is increasingly used over sub-continental to continental regions.[3-9] Similarly, dispersion or chemical transport modelling has been used in conjunction with LUR in so-called hybrid models.[10-12] Because of the often relatively coarse spatial resolution of the data (~10x10km), both satellite-derived (SAT) and chemical transport model (CTM) estimates represent area-averaged concentrations. Both also take into account the formation of secondary components with chemical transformations. Integrating satellite derived and/or chemical transport model estimates within LUR may help to achieve a better prediction of air pollution exposure in large-area or even continent-wide studies. Few studies have assessed whether the combination of satellite-based and chemical transport model estimates can help better explain the spatial variation of air pollution concentrations.[13]

This study presents a comparative assessment of models aimed at characterising air pollution concentrations in Europe through harmonised methods at the local scale for future use in population health studies. In a LUR framework, we combine European-wide satellite-derived ground-level concentration estimates, outputs from a chemical transport model and land use predictors with two ground-based monitoring datasets; the European AIRBASE network[13] and the ESCAPE (European Study of Cohorts for Air Pollution Effects) measurement sites.[14,15] We focus on the pollutants NO_2 and $PM_{2.5}$.

2. Methods

Study area

The study area consists of 19 European countries with available measurements in the AIRBASE dataset (see Figure 1), the majority of which were part of the ESCAPE project.[14,15] Measurement and geospatial predictor data were processed in GIS after being (re)projected into the European Terrestrial Reference System (ETRS Lambert Azimuthal Equal Area 52 10), also used for the European Environment Agency (EEA) reference grid.

Air pollution monitoring data

Air pollution monitoring data were used from the ESCAPE study and the AIRBASE database held by the European Environmental Agency.[14]

We used the ESCAPE annual mean concentrations reflecting the period 2009-2010 from 1426 sites in 36 study areas for NO_2 and 436 sites in 20 study areas for $PM_{2.5}$ (Figure 1). The ESCAPE measurement campaign was designed specifically to investigate relationships between long term exposure to air pollution and health in existing cohort studies using a land use regression approach. As such, the measurements were undertaken in the relevant study areas of the cohorts. Detailed information about the measurement campaign including site selection and measurement methods can be found elsewhere.[15,16] In brief, over the period of one year (either 2009 or 2010), three 2-weekly measurement campaigns were held in all the study areas measuring $PM_{2.5}$ (20 sites per area) and/or NO_2 (40 sites per area) using Harvard Impactors and Ogawa badges respectively. A previous analysis showed that there was less than 1 $\mu g/m^3$ difference in overall AIRBASE NO_2, $PM_{2.5}$ and PM_{10} annual average concentrations between 2009 and 2010.[15,16] We therefore assumed all ESCAPE measurements to be representative for 2010 in line with all the other data we obtained (AIRBASE $PM_{2.5}$ and NO_2, SAT and CTM). The 3 monitoring periods were held: one in the cool (winter), warm (summer) and intermediate season (autumn or spring) to capture seasonality. One reference monitor in each study period was run during the whole year and these measurements were used to calculate an adjusted annual mean of the measured pollutant concentrations at every site location.

Annual mean concentrations for $PM_{2.5}$ (549 sites) and NO_2 (2400 sites) for 2010 were also derived from the AIRBASE v8 dataset (Figure 1).[14] An annual average was only calculated when a site captured ≥75% of the total hours (NO_2) and days ($PM_{2.5}$).

Table 1 describes summary statistics of the measured concentrations for the ESCAPE and AIRBASE datasets. Site types and their distribution differed between the AIRBASE and ESCAPE datasets. AIRBASE includes “background”, “industrial” and “traffic” sites, all of which are included here. ESCAPE site locations, classified as “regional background”, “urban background” and “traffic”, were selected to represent population exposures within the ESCAPE study areas, and thus traffic sites were overrepresented.

We randomly stratified both sets of monitoring data by region (defined below) and site type and created a derivation (80%) and a validation (20%) set. We performed the stratification six times and selected the stratification where all the strata where significant (P-value > 0.1). For NO_2 the study areas were divided into five regions (North, West, Central, South West, South East). For $PM_{2.5}$ four regions were chosen to have a sufficient number of sites in each (North, West, Central, South). Table S1 summarises the measured concentrations by region.

Satellite derived air pollution estimates

Satellite derived (SAT) estimates of $PM_{2.5}$ for Europe were extracted from the global datasets reported in van Donkelaar et al.[17] These $PM_{2.5}$ estimates relate aerosol optical depth (AOD) retrievals from the NASA MODIS (Moderate Resolution Imaging Spectroradiometer), MISR (Multi-angle Imaging Spectroradiometer) and SeaWiFS instruments to near-surface concentrations using aerosol vertical profiles and scattering properties simulated by the GEOS-Chem chemical transport model. A dataset for the year 2010 (inferred from 2009 – 2011) was obtained at a 0.1° x 0.1° (~10km) resolution.

For NO_2, satellite derived estimates were obtained from the tropospheric NO_2 columns measured with the OMI (Ozone Monitoring Instrument) on board the Aura satellite. Similar to

$PM_{2.5}$, the satellite column-integrated retrievals were related to ground-level concentrations using global GEOS-Chem model, producing an annual gridded NO_2 surface for the year 2010 at a 10km resolution.[3,8,18]

Chemical transport model estimates

Long range chemical transport model (CTM) estimates for $PM_{2.5}$ and NO_2 were derived from the MACC-II ENSEMBLE model, for the year 2010 at 0.1° x 0.1° (~10km) resolution, with estimates available across the whole study area.[19] At each pixel, the ENSEMBLE model value was defined as the median value of the following seven individual regional CTMs at that particular point: CHIMERE, EMEP, EURAD, LOTOS-EUROS, MATCH, MOCAGE and SILAM. The obtained NETCDF files were imported in ArcGIS for further processing.

Other predictor variables (Roads, land cover, altitude, north-south/east-west trend)

A spatial moving window summation function (focalsum in ArcGIS10) was used to calculate the local predictor variables (e.g. length of road and areas of different land covers) for selected distances around the sites (Table S2). More details about these data can be found in Vienneau et al.[4] Briefly, road data originated from the 1:10,000 EuroStreets digital road network (version 3.1, based on TeleAtlas MultiNet TM for year-2008). The road data was classified into 'all' and 'major' roads using the classification available in EuroStreets. These were then intersected with a 100m base polygon and the sum of road length within each 100x100m cell calculated and converted into a 100m grid. For land cover, the 100m European Corine Land Cover 2006 data set was obtained.[20] This dataset covered the whole study area except Greece. For Greece, the dataset for year 2000 was used.[21] From the available 44 land classes, six main groups were derived: residential (proxy for population density and domestic sources of air pollution), industry, ports, urban green space, total built up and natural land. For elevation we use the SRTM Digital Elevation Database version 4.1 with a resolution of one arc second (approximately 90 m) and a vertical error <16 m. [22] SRTM is available for most of the study area, up to 60°N latitude. For northern Scandinavia we used the 1km resolution Topo30 data. The predictor variable grid reflecting north-south trend was constructed by taking the Y-coordinate (centroids) of the 100x100m basegrid.

Statistical analysis

Geospatial analysis was performed in ESRI ArcGIS 10 and statistical analysis in SPSS version 23.

Models were developed for $PM_{2.5}$ and NO_2 based on the ESCAPE and AIRBASE measurement datasets separately. Because of the differences between the ESCAPE and AIRBASE monitoring data (see Discussion), we refrained from developing models combining the two datasets. Following the ESCAPE protocol,[23] supervised stepwise linear regression was used to predict concentrations at measurements sites on the basis of the available predictor variables. For each pollutant the following four LUR models at ESCAPE and AIRBASE sites were developed:

1. no SAT or CTM estimates (M1);
2. forcing in SAT estimates (M2);
3. forcing in CTM estimates (M3);
4. forcing in both SAT and CTM estimates (M4).

Models were developed using 80% of the sites and validated on the remaining 20%, the hold-out-validation (HOV) set. Predictor variables were only maintained in the model if they followed the expected direction of effect (e.g. positive for SAT, CTM, road length and negative for green space and natural areas). We did not follow the rule previously used in the ESCAPE protocol, i.e. that variables had to add more than 1% to the adjusted R^2. Instead the addition of variables was repeated until no variable added to the adjusted R^2 of the previous model. This allowed significant predictors to enter the model which would have otherwise been ruled out. Compared to earlier ESCAPE analyses within study areas, we now analysed more sites and exploited much larger variation in measured concentrations. The latitude and longitude variables were only offered to the models if other variables were exhausted. Models were checked for co-linearity (VIF) and influential observations (Cook's D). Every model was also validated using the monitoring data not used in model building; i.e. ESCAPE models were validated at the complete set of AIRBASE monitoring sites and vice versa (cross-over-validation, COV). We additionally performed cross-over validation at just the HOV dataset of the other dataset (cross-over-hold-out-validation, COHOV) to compare the performance of the ESCAPE and AIRBASE models.

For the validations (HOV, COV and COHOV) we calculated the following performance statistics: R^2, RMSE, the constant and slope of the regression line, and additionally for HOV: mean error (ME), absolute error (AE), mean bias (MB), absolute bias (AB) and fractional bias (FB). For insight into suitability of models to estimate exposures for cohorts in smaller regions, we also evaluated model performance at the regional level using R^2, RMSE, constant and slope. The performance of models was also evaluated by site type (R^2, RMSE) to investigate possible bias by monitoring location characteristics.

To compare the separate contribution of predictor variables in the models, the regression slope (ß) of each variable was multiplied by the difference between the 95th and 5th percentile of each predictor value (predicted P95-P5 in $\mu g/m^3$).

For the purpose of this assessment we defined squared correlations (R^2) as weak (0 - 0.2), moderate (>0.2 – 0.4), moderately strong (>0.4 – 0.6) and strong (> 0.6).

3. Results

Correlation measured concentration, SAT and CTM

$PM_{2.5}$ SAT estimates have a moderately strong association with measured $PM_{2.5}$ concentrations at ESCAPE and AIRBASE sites (Figure S1, R^2 = 0.44 and 0.49 respectively). $PM_{2.5}$ CTM estimates show a similar correlation at AIRBASE sites (R^2 = 0.40) but less so at ESCAPE sites (0.22). $PM_{2.5}$ SAT and $PM_{2.5}$ CTM are weakly correlated at ESCAPE sites and moderately strong at AIRBASE sites. The weak association seems partially caused by a number of sites in Paris were CTM estimates are nearly 2 to 3 times higher than SAT estimates and higher than the ground measurements.

NO_2 CTM estimates and especially NO_2 SAT estimates are less successful in explaining the variation in measured NO_2 concentrations. SAT and CTM estimates are moderately strongly correlated, although CTM estimates are more than 3 times higher than SAT at both AIRBASE and ESCAPE sites.

$PM_{2.5}$ models

The M1 models without satellite and chemical transport model estimates performed moderately, explaining 38% (33%) of the variation in measured $PM_{2.5}$ concentrations during the model derivation at the ESCAPE (AIRBASE) sites (Table 2). The models are dominated by non-traffic variables (e.g. urban green, natural, y-coordinate). The M2 models, including the SAT estimate, performed better, explaining 58% (ESCAPE) and 61% (AIRBASE) of the observed variation. In both ESCAPE and AIRBASE M2 models, the SAT variable has the largest contribution (partial R^2: 0.45 and 0.48, P95-P5: 10.99 and 10.18 µg/m^3) (Table S3). Despite improving the partial R^2 only slightly, local traffic indicators with small buffer sizes enter the models, explaining some of the residual local variation in $PM_{2.5}$ concentrations. Including the CTM estimate (M3) also produced better models, especially at AIRBASE sites where we observe a higher derivation R^2 (adj R^2 = 0.52) than model M1. The ESCAPE M3 model performs less well (derivation adj R^2 = 0.40). The CTM variable had the largest influence in the AIRBASE M3 model (P95-P5 = 10.49 µg/m^3). This was not the case in the ESCAPE model, where the y-coordinate took the largest share (P95-P5 = -7.38 µg/m^3). The best predictive models for $PM_{2.5}$ at ESCAPE and AIRBASE sites included both SAT and CTM estimates (M4). The M4 ESCAPE and AIRBASE models explained about 2% more variation than the models with SAT only. Local predictor variables retained in the ESCAPE model included two local road variables (major roads, all roads 100m), residential area, altitude and y-coordinate. The AIRBASE model was very similar also including a local road variable (major roads 100m).

Overall, model HOV R^2 was 5-8% lower than the derivation R^2 suggesting robust models. All validation statistics (HOV, COV and COHOV) showed the same pattern as the model R^2: ESCAPE and AIRBASE M2 and M4 models were consistently better than the respective M1 and M3 models (Tables 2 and S4). Importantly, the M4 models explained 52 to 59% of the variation in the other dataset (COV validation), which is almost equal to the respective HOV R^2, further supporting the robustness of the models.

The AIRBASE M4 $PM_{2.5}$ model was applied to the whole study area at a 100m resolution (Figure 2). The map shows generally lower estimated $PM_{2.5}$ concentrations in the north than in the south. Large conurbations like Paris (France) and London (UK) can be detected, as can large industrial regions like the Po valley (Italy) and the Ruhr area (Germany). On closer inspection (see inset) the influence of the larger scale predictor variables from the satellite model becomes apparent. Also apparent are the cells with ‘no data’ as a result of the grid cells without a satellite estimate. The transect graph illustrates that the $PM_{2.5}$-SAT and $PM_{2.5}$-CTM variables contribute most to the predicted $PM_{2.5}$ concentration, with variables like major roads and residential area adding to the local variation (Figure 2). The scatterplots show the moderately strong correlation for both HOV and COV validations. Regression lines are close to the 1:1 line (Table S4).

NO_2 models

The M1 models without satellite and chemical transport model estimates performed moderately strong, explaining 47 and 52% of the variation in measured NO_2 concentrations at the ESCAPE and AIRBASE sites respectively (Table 2). The ESCAPE and AIRBASE models with CTM explained 7-10% more variation than the models without SAT or CTM, more than the models with SAT (2-4% additional explained variance). All 3 ESCAPE models

(M1, M2 and M3) included similar predictor variables like length of major road and all roads and residential area within different buffers and y-coordinate, with M1 and M2 also including ports and industrial/commercial area. CTM was by far the strongest variable in ESCAPE M3 (P95-P15 = 24.83 µg/m^3) (Table S3). In the AIRBASE M3 model CTM and length of all roads within 2km were strongly influential (P95-P5 = 17.25 and 11.95 µg/m^3 respectively). Forcing SAT and CTM together in M4 caused the coefficient of the satellite predictor to become negative, invalidating both the ESCAPE and AIRBASE models.

In cross-over validation, the ESCAPE model M3 explained 55% (COV) of the measured variation at the AIRBASE sites, whereas the AIRBASE M3 model explained 50% at the ESCAPE sites (Table 2). As observed for $PM_{2.5}$, the COV R^2 was similar to the HOV R^2 determined within each respective dataset.

Figure S2 shows the NO_2 M3 AIRBASE model (highest derivation R^2 and HOV R^2) applied to the study area at 100m resolution. Individual cities show up with higher estimated NO_2 concentrations. Additionally, the influence of the road predictor variables clearly shows up in the inset. The transect shows how the NO_2 CTM variable builds the regional variation and the roads and residential predictors add the local (i.e. spikey) variation. Scatterplots of the HOV and COV validation show moderately strong correlations and regression lines almost 1:1.

Model performance at subcontinental level and by site type

$PM_{2.5}$ M4 and NO_2 M3 (ESCAPE and AIRBASE), performed moderately to strong in all regions for the COV validation (Table S5, R^2 0.30 to 0.75). Equally, the performance of these models were similar for the different site types for both the HOV and COV validation (Table S6, R^2 0.32 to 0.72), except for a lower explained variance of both NO_2 models for traffic sites. Here the lack of traffic intensity data and street configuration data may have played a role.

Sensitivity analysis

As a sensitivity analysis we developed models based on combined AIRBASE and ESCAPE derivation sites (80%), adding an indicator for network as the last predictor. Similar to the main models, this was validated with a 20% HOV. We performed this test for $PM_{2.5}$ M4 (including both SAT and CTM) and NO_2 M3 (including CTM), finding very similar results to the main models (see Table S7). The indicator variable for network was significant in both models, providing empirical evidence against combining the monitoring datasets.

4. Discussion

We assessed the contribution of satellite or chemical transport modelling data to Europe-wide long-term $PM_{2.5}$ and NO_2 land use regression models using two monitoring databases. Satellite and chemical transport model estimates added to LUR models increased the explained spatial variation of measured air pollution concentrations separately ($PM_{2.5}$ and NO_2) and together ($PM_{2.5}$).

$PM_{2.5}$ models including both satellite and chemical transport model estimates performed best at both monitoring datasets: 20-30% additional variance explained compared to models with only land use and traffic variables. The satellite component had the largest contribution to

the overall predicted $PM_{2.5}$ concentrations. For NO_2 the best models included the chemical transport model estimates (6-10% additional explained variance). Validation of models within the same monitoring dataset and across monitoring datasets suggested robust models.

ESCAPE versus AIRBASE

There was little difference between the overall performance of the ESCAPE and AIRBASE models for both pollutants. Also the HOV, COV and COHOV validations showed similar results. This is remarkable, given the differences between the ESCAPE and AIRBASE monitoring datasets. Figure 1 shows the striking difference in spatial coverage of the monitoring networks. The ESCAPE monitoring sites are located in 20 study areas for $PM_{2.5}$ and 36 areas for NO_2, with only the Netherlands having a near national coverage. The AIRBASE monitoring sites, on the contrary, are more evenly spread across the countries. Another difference between the two datasets is the number of sites, which for both pollutants is larger for AIRBASE than ESCAPE (2400 versus 1436 [NO_2]; 549 versus 436 [$PM_{2.5}$]). A crucial difference is the location of the monitoring sites in relation to residential exposure. The choice of the location of monitoring sites in the ESCAPE study was purposely designed such that it would best reflect the spatial variation of air pollution exposures among the cohort study populations within each ESCAPE study area, without the explicit aim to cover Europe as a whole. The monitoring locations in the regulatory AIRBASE network are chosen on a different principle, namely to check for breaches of the air quality guidelines at background sites, near busy roads or in industrial zones. Another important difference is the sampling method used in the two networks. In the ESCAPE study, a harmonised study protocol was implemented based on the Harvard impactor (gravimetry) to monitor $PM_{2.5}$ and the Ogawa badge (diffusion) for NO_2. Because the AIRBASE network is a collection of sites from national networks, the measurement techniques and equipment can differ although reference methods do exist. The most common AIRBASE measurement technique for NO_2 was chemiluminescence, with a minority of AIRBASE sites using Griess-Saltzman reaction, chromatography or diffusion from a variety of monitoring equipment. $PM_{2.5}$ measurements in AIRBASE were carried out mainly by beta ray attenuation or gravimetry, with some sites using TEOM and light scattering devices. Because of the above mentioned differences we refrained from developing models combining the two datasets.

Despite these differences, the two different monitoring datasets performed very similarly in terms of explained variation in monitored concentrations predictor variables and regression coefficients. Also the performance of the best models tested on the opposite monitoring sites were adequate (COV = 50-59%, HOCOV = 43-53%), giving weight to the robustness of the models developed here. This finding is of high relevance for future air pollution and health research in Europe. AIRBASE data are available in the long term, and our results indicate that future epidemiological studies may rely on these routine data for regulated air pollutants to model exposure distributions within and across European cities.

In the majority of models (12 out of 14), y coordinate was included as an influential predictor variable, reflecting the North (lower) to South (higher) trend in the measured concentrations at both ESCAPE and AIRBASE monitoring sites. This is likely caused by a combination of higher source / population density, emission factors and a generally warmer and drier climate in the South and the influence of Sahara dust in the Mediterranean area.

Application of the ESCAPE model to epidemiological studies in study areas not covered by the original study areas, may be associated with additional misclassification of exposure. The good performance of the ESCAPE model to predict concentrations at AIRBASE sites, covering a large number of regions not covered by ESCAPE monitoring, suggest this may not be a major issue.

SAT versus CTM

$PM_{2.5}$ SAT estimates fitted much better to measured data, both at the ESCAPE and AIRBASE monitoring sites, than the CTM model and consistently improved LUR models more than CTM. Similar comparison results, using satellite-derived $PM_{2.5}$ estimates, were found by van Donkelaar et al.[17] indicating a R^2 of 0.53 between the $PM_{2.5}$ SAT surfaces and European Monitoring and Evaluation Programme (EMEP) measurements from 2001 to 2010. Our correlation is lower because EMEP sites are predominantly located at regional background.

In contrast, for NO_2, CTM correlated better with the measurements and contributed more to the LUR model performance. The difference between $PM_{2.5}$ and NO_2 might be explained by better performance of CTM for the gaseous component NO_2 than for fine particles. $PM_{2.5}$ is a complex pollutant, consisting of primary and secondary particles, and therefore with probably less well-characterized emission input data. This is supported by the overestimation of $PM_{2.5}$ by CTM in the Paris region, contributing to a weak correlation between CTM and $PM_{2.5}$ measurements in the ESCAPE data. The spatial scale of SAT and CTM was similar at about 10*10 km, so neither method predicted well the small-scale spatial variation related to local sources.

While for $PM_{2.5}$, the inclusion of CTM (M4) improved the LUR model with SAT (M1) slightly, for NO_2, SAT (M2) did not provide any additional prediction to models with CTM (M3). The correlation between SAT and CTM estimates is stronger for NO_2 than for $PM_{2.5}$, especially at the ESCAPE sites.

The NO_2 model estimates underestimated the measured concentrations at the ESCAPE and AIRBASE modelling sites with between 10 (CTM) and 20 (SAT) $\mu g/m^3$ (Figure S1). Underestimation of the 2010 NO_2 MACC data is also reported by Giordano et al.,[24] showing a consistent underestimation of the MACC model compared to surface NO_2 concentrations at 285 rural stations across Europe. They speculated that this could be due to underestimated emissions in the inventories used by the MACC re-analysis, as well as an underestimation of the chemical lifetime of NOx, too high modelled dry deposition and an underestimation of the natural emissions from soils and/or lightning. Another explanation they offer is the possible systematic positive bias of the NO_2 measurements, i.e. for some instruments only 70-83% of the actual measured NO_2 is attributable to real NO_2.[24] By offering both the spatially coarse CTM estimates and variables which simulate emission sources at a more detailed resolution, the ESCAPE and AIRBASE LUR models can add to the overall R^2 of the CTM model, as shown here, by 20 to 30% respectively. This is also illustrated in the transect (Figure S2) where the CTM provides an area-averaged surface that is dominated by the regional background, on top of which the local variables add the necessary more local variation.

The underestimation of NO_2 SAT (~20 µg/m^3) was also reported by Vienneau et al.[4] for the years 2005 to 2007, when comparing with NO_2 measurements at over 2000 AIRBASE sites in Europe. A similar finding was reported by Bechle et al.[18] for the South Coast Air Basin of California (USA) where the difference between NO_2 SAT and measured NO_2 in 2005 was around 10 ppb (~19 µg/m^3) and by Kharol et al.[25] who report absolute concentrations from in situ measurements in North America where twice those from satellite-derived estimates. This is not surprising as the coarse scale satellite-derived NO_2 estimates are area-averaged concentrations, while NO_2 monitors represent the concentration at a specific point, often at roadside or close to city centres. Similarly as with the NO_2 CTM data, the difference was made up by predictor variables representing local sources.

SAT and CTM improved $PM_{2.5}$ models based on land use/traffic variables more than the NO_2 models. This is consistent with the larger impact of variation of the (regional) background on concentrations of $PM_{2.5}$ compared NO_2. For the ESCAPE monitoring data, we previously reported that 81% of total variance of $PM_{2.5}$ was between study area variance, whereas for NO_2 40% was between and 60% within study area variance.[15,16] The differences are a result of the magnitude of local sources, atmospheric formation and loss processes and the resulting atmospheric lifetime of components.

Comparison with other continental models

It has been previously shown that the inclusion of satellite data improved model performance of European-wide LUR models for NO_2 and PM_{10} respectively by 0.05 and 0.11, explaining 46-56% of the variation in annual means for NO_2 and 36-48% of PM_{10}.[4] At the time of this previous study, it was not possible to develop $PM_{2.5}$ models due to the sparseness of $PM_{2.5}$ monitoring data (195 sites operating in Western Europe during 2007). Recently, however, there has been a sharp increase in the number of $PM_{2.5}$ monitoring sites; 549 sites with >75% annual data capture operating in 2010 (AIRBASE). At the same time, the ESCAPE study undertook a monitoring campaign measuring $PM_{2.5}$ at 436 sites across Europe. Compared to the NO_2 models described in Vienneau et al.[4], using AIRBASE and similar GIS predictor variables as used here, the performance of our models developed here are similar; no direct comparison between the PM models was possible, however our best $PM_{2.5}$ models outperform the previous PM_{10} models by more than 10% (36-48% v 60-63%). No other high resolution air pollution models are available for Europe as a whole. Authors have developed models in North America with similar performance results. Hystad et al.[26] developed $PM_{2.5}$ and NO_2 models using satellite-based estimates explaining respectively 52% and 38% of measured spatial variation in Canada for the time period 1975 to 1994. They compensated for the lack of historical $PM_{2.5}$ measurements, which only started in 1984, by developing predictive models based on co-located $PM_{2.5}$ and Total Suspended Particles (started in 1970) measurements from 1984 to 2000 to predict $PM_{2.5}$ concentrations back to 1974. Van Donkelaar et al.[9] developed a model that combined geographic weighted regression with satellite-based estimates to explain 82% of the measured spatial variation in $PM_{2.5}$ for North America for 2004-2008. A similar study in the USA by Novotny et al.[3] also incorporating satellite-based estimates developed a national NO_2 model explaining 78% of the concentrations measured in 2006. Models for North America may perform better than ours because measured concentrations are generally lower and show less variability and are therefore less sensitive to missing predictor variables representing local sources.

Wang et al.[27] also used the ESCAPE monitoring dataset to build $PM_{2.5}$ and NO_2 models at European scale. It is important to note the difference in modelling approaches between Wang et al.[27] and this study. Wang et al.[27] used all available ESCAPE predictor variables including local sourced variables like traffic intensity. Despite traffic intensity being available also in areas outside the ESCAPE study areas, within the scope of this study it was not possible to source these separately, and for this reason we could not use these local predictor variables. Despite this, the NO_2 models in both studies are comparable in terms of explained variation (56% in Wang, 58% here). For $PM_{2.5}$, Wang et al.[27] obtained a higher explained variance, $R^2 = 0.80$, compared to $R^2 = 0.59$ to 0.63 here. The better $PM_{2.5}$ model performance by Wang et al.[27] was driven by the inclusion of measured regional background concentration, something which was not possible at the scale of this study.

Limitations

No traffic data is available in the whole European study area, so we have used road length for major and all roads as a proxy for traffic sources. The resolution of the SAT and CTM estimates available to us at the time of the study is coarse (~10x10km). Efforts are taking place to refine the resolution to 3 or 1km grids, which, in future, will help increase the performance of the predictive models. The $PM_{2.5}$ SAT data has cells with missing values, especially in high altitude areas (Alps, Pyrenees, Norway) and over water bodies (Sweden), which is apparent in Figures 2 and S2. Although these areas typically have a low population density, this is something to keep in mind when using the data in subsequent health analysis.

In summary we found that satellite-derived estimates contribute considerably to the explained variance in $PM_{2.5}$ measured at both ESCAPE and AIRBASE sites. For NO_2, the estimates produced by a chemical transport model improve model predictions compared to a models based only on local and satellite-derived data. Either of the large scale predictors (SAT, CTM) can help produce better continental scale LUR models.

The comparison between measurement data from the routine and purpose-designed monitoring network show that both networks are useful for producing models explaining the spatial variance over a large study area. Especially encouraging is that models based on routine monitoring data are sufficient to predict air pollution exposures at the ESCAPE monitoring sites, with the prospect of future model development for regulated and routinely measured air pollutants. Dedicated measurement campaigns will be required to assess very small-scale differences in exposure and health effects of unregulated air quality indicators.

The resulting $PM_{2.5}$ and NO_2 surfaces at 100x100m resolution will be made available for the large scale epidemiological studies. To our knowledge, this is the first detailed surface of annual mean $PM_{2.5}$ produced for large parts of Europe. Together with the NO_2 surface the data will be made freely available to the research community to facilitate further epidemiological research.

Associated Content

Supplemental Information

Tables S1, Descriptive statistics monitoring data by region; S2, GIS predictor variables; S3, Model building statistics; S4, Performance statistics; S5, Performance indicators for

validation sets; S6, Performance of models at subcontinental level; S7, Model building statistics for combined models. Figures S1, Scatterplots between $PM_{2.5}$ and NO_2 concentrations, SAT and CTM at ESCAPE and AIRBASE sites; S2, Map NO_2 M3 AIRBASE, 2010

Acknowledgements/Funding

The research was supported by funding from the European Community's Seventh Framework Program EXPOsOMICS and ESCAPE studies under grant agreement numbers: FP7 308610 and FP7 211250 respectively. The Air quality modelling data were produced within MACC projects funded by the European Commission under the EU Seventh Research Framework Programme (grant agreement no. 283576, MACC II).

References

1. Pedersen, M.; Giorgis-Allemand, L.; Bernard, C.; Aguilera, I.; Andersen, A. M.; Ballester, F.; Beelen, R. M.; Chatzi, L.; Cirach, M.; Danileviciute, A.; Dedele, A.; van Eijsden, M.; Estarlich, M.; Fernandez-Somoano, A.; Fernandez, M. F.; Forastiere, F.; Gehring, U.; Grazuleviciene, R.; Gruzieva, O.; Heude, B.; Hoek, G.; de Hoogh, K.; van den Hooven, E. H.; Haberg, S. E.; Jaddoe, V. W.; Klümper, C.; Korek, M.; Krämer, U.; Lerchundi, A.; Lepeule, J.; Nafstad, P.; Nystad, W.; Patelarou, E.; Porta, D.; Postma, D.; Raaschou-Nielsen, O.; Rudnai, P.; Sunyer, J.; Stephanou, E.; Sorensen, M.; Thiering, E.; Tuffnell, D.; Varro, M. J.; Vrijkotte, T. G.; Wijga, A.; Wilhelm, M.; Wright, J.; Nieuwenhuijsen, M. J.; Pershagen, G.; Brunekreef, B.; Kogevinas, M.; Slama, R. Ambient air pollution and low birthweight: a European cohort study (ESCAPE). *Lancet Respir. Med*. **2013**, 1, 695-704.
2. Beelen, R.; Raaschou-Nielsen, O.; Stafoggia, M.; Andersen, Z. J.; Weinmayr, G.; Hoffmann, B.; Wolf, K.; Samoli, E.; Fischer, P.; Nieuwenhuijsen, M.; Vineis, P.; Xun, W. W.; Katsouyanni, K.; Dimakopoulou, K.; Oudin, A.; Forsberg, B.; Modig, L.; Havulinna, A. S.; Lanki, T.; Turunen, A.; Oftedal, B.; Nystad, W.; Nafstad, P.; de Faire, U.; Pedersen, N. L.; Östenson, C. G.; Fratiglioni, L.; Penell, J.; Korek, M.; Pershagen, G.; Eriksen, K. T.; Overvad, K.; Ellermann, T.; Eeftens, M.; Peeters, P. H.; Meliefste, K.; Wang, M.; Bueno-de-Mesquita, B.; Sugiri, D.; Krämer, U.; Heinrich, J.; de Hoogh, K.; Key, T.; Peters, A.; Hampel, R.; Concin, H.; Nagel, G.; Ineichen, A.; Schaffner, E.; Probst-Hensch, N.; Künzli, N.; Schindler, C.; Schikowski, T.; Adam, M.; Phuleria, H.; Vilier, A.; Clavel-Chapelon, F.; Declercq, C.; Grioni, S.; Krogh, V.; Tsai, M. Y.; Ricceri, F.; Sacerdote, C.; Galassi, C.; Migliore, E.; Ranzi, A.; Cesaroni, G.; Badaloni, C.; Forastiere, F.; Tamayo, I.; Amiano, P.; Dorronsoro, M.; Katsoulis, M.; Trichopoulou, A.; Brunekreef, B.; Hoek, G. Effects of long-term exposure to air pollution on natural-cause mortality: an analysis of 22 European cohorts within the multicentre ESCAPE project. *Lancet*. **2014**, 383, 785-795.
3. Novotny, E. V.; Bechle, M. J.; Millet, D. B.; Marshall, J. D. National satellite-based land-use regression: NO_2 in the United States. *Environ. Sci. Technol.* **2011**, 45 (10), 4407−4414.
4. Vienneau, D.; de Hoogh, K.; Bechle, M. J.; Beelen, R.; van Donkelaar, A.; Martin, D. B.; Millet, D. B.; Hoek, G.; Marshall, J. D. Western European land use regression

incorporating satellite- and ground-based measurements of NO2 and PM10. *Environ. Sci. Technol.* **2013**, 47 (23), 13555−13564.

5. van Donkelaar, A.; Martin, R. V.; Brauer, M.; Kahn, R.; Levy, R.; Verduzco, C.; Villeneuve, P. J. Global estimates of ambient fine particulate matter concentrations from satellite-based aerosol optical depth: Development and application. *Environ. Health Perspect*. **2010**, 118 (6), 847−855
6. Kloog, I.; Nordio, F.; Coull, B. A.; Schwartz, J. Incorporating local land use regression and satellite aerosol optical depth in a hybrid model of spatiotemporal $PM_{2.5}$ exposures in the Mid-Atlantic States. *Environ. Sci. Technol.* **2012**, 46 (21), 11913−11921.
7. Ma, Z.; Hu, X.; Huang, L.; Bi, J.; Liu, Y. Estimating Ground-Level $PM_{2.5}$ in China Using Satellite Remote Sensing. *Environ. Sci. Technol.* **2014**, 48 (13), 7436-7444.
8. Bechle, M.; Millet, D. B.; Marshall, J. D. National Spatiotemporal Exposure Surface for NO_2: Monthly Scaling of a Satellite-Derived Land-Use Regression, 2000−2010. *Environ. Sci. Technol.* **2015**, 49, 12297−12305.
9. van Donkelaar, A.; Martin R. V.; Spurr R. J. D.; Burnett R. T. High-resolution satellite-derived $PM_{2.5}$ from optimal estimation and geographically weighted regression over North America, *Environ. Sci. Technol.* **2015a**, 49 (17), 10482–10491.
10. Wilton, D.; Szpiro, A.; Gould, T.; Larson, T. Improving spatial concentration estimates for nitrogen oxides using a hybrid meteorological dispersion/land use regression model in Los Angeles, CA and Seattle, WA. *Sci. Tot. Environ.* **2010**, 408, 1120-1130.
11. Arain, M. A.; Blair, R.; Finkelstein, N.; Brook, J. R.; Sahsuvaroglu, T.; Beckerman, B.; Zhang, L.; Jerrett, M. The use of wind fields in a land use regression model to predict air pollution concentrations for health exposure studies. *Atm. Environ.* **2007**, 41, 3453-3464.
12. Akita, Y.; Baldasano, J. M.; Beelen, R.; Cirach, M.; de Hoogh, K.; Hoek, G.; Nieuwenhuijsen, M.; Serre, M. L.; de Nazelle, A. Large Scale Air Pollution Estimation Method Combining Land Use Regression and Chemical Transport Modeling in a Geostatistical Framework. *Environ. Sci. Technol.* **2014**, 48, 4452-4459.
13. Reid, C. E.; Jerrett, M.; Petersen, M. L.; Pfister, G. G.; Morefield, P. E., Tager, I. B.; Raffuse, S. M.; Balmes, J. R. Spatiotemporal prediction of fine particulate matter during the 2008 northern California wildfires using machine learning. *Environ Sci Technol.* **2015**, 49, 3887-3896.
14. EEA AirBase - The European air quality database, version 8. http://www.eea.europa.eu/data-and-maps/data/airbase-the-european-air-quality-database-8 Access (13 January 2015)
15. Cyrys, J.; Eeftens, M.; Heinrich, J.; Ampe, C.; Armengaud, A.; Beelen, R.; Bellander, T.; Beregszaszai, T.; Birk, M.; Cesaroni, G.; Cirach, M.; de Hoogh, K.; de Nazelle, A.; de Vocht, F.; Declercq, C.; Dedele, A.; Dimakopoulou, K.; Eriksen, K.; Galassi, C.; Grazuleviciene, R.; Grivas, G.; Gruzieva, O.; Hagenbjörk Gustafsson, A.; Hoffmann, B.; Iakovides, M.; Ineichen, A.; Krämer, U.; Lanki, T.; Lozano, P.; Madsen, C.; Meliefste, K.; Modig, L.; Mölter, A.; Mosler, G.; Nieuwenhuijsen, M.; Nonnemacher, M.; Oldenwening, M.; Peters, A.; Pontet, S.; Probst-Hensch, N.; Quass, U.; Raaschou-Nielsen, O.; Ranzi, A.; Sugiri, D.; Stephanou, E. G.; Taimisto, P.; Tsai, M. Y.; Vaskövi, E.; Villani, S.; Wang, M.; Brunekreef, B.; Hoek, G. Variation of NO2 and NOx concentrations between and within 36 European study areas: results from the ESCAPE study. *Atmos. Environ*. **2012**, 62, 374-390.

16. Eeftens, M.; Tsai, M.-Y.; Ampe, C.; Anwander, B.; Beelen, R.; Bellander, T.; Cesaroni, G.; Cirach, M.; Cyrys, J.; de Hoogh, K.; De Nazelle, A.; de Vocht, F.; Declercq, C.; Dėdelė, A.; Eriksen, K.; Galassi, C.; Gražulevičienė, R.; Grivas, G.; Heinrich, J.; Hoffmann, B.; Iakovides, M.; Ineichen, A.; Katsouyanni, K.; Korek, M.; Krämer, U.; Kuhlbusch, T.; Lanki, T.; Madsen, C.; Meliefste, K.; Mölter, A.; Mosler, G.; Nieuwenhuijsen, M.; Oldenwening, M.; Pennanen, A.; Probst-Hensch, N.; Quass, U.; Raaschou-Nielsen, O.; Ranzi, A.; Stephanou, E.; Sugiri, D.; Udvardy, O.; Vaskövi, É.; Weinmayr, G.; Brunekreef, B.; Hoek, G. Spatial variation of PM2.5, PM10, PM2.5 absorbance and PMcoarse concentrations between and within 20 European study areas and the relationship with NO2 − Results of the ESCAPE project. *Atmos. Environ.* **2012a**, 62, 303−317.
17. van Donkelaar, A.; Martin, R. V.; Brauer M.; Boys B. L. Use of Satellite Observations for Long-Term Exposure Assessment of Global Concentrations of Fine Particulate Matter. *Environ. Health Perspect*. **2015b**, 123, 135–143.
18. Bechle, M. J.; Millet, D. B.; Marshall, J. D. Remote sensing of exposure to NO2: satellite versus ground-based measurement in a large urban area. *Atmos. Environ.* **2013**, 69 (2), 345−353.
19. Inness, A.; Baier, F.; Benedetti, A.; Bouarar, I.; Chabrillat, S.; Clark, H.; Clerbaux, C.; Coheur, P.; Engelen, R. J.; Errera, Q.; Flemming, J.; George, M.; Granier, C.; Hadji-Lazaro, J.; Huijnen, V.; Hurtmans, D.; Jones, L.; Kaiser, J. W.; Kapsomenakis, J.; Lefever, K.; Leitão, J.; Razinger, M.; Richter, A.; Schultz, M. G.; Simmons, A. J.; Suttie, M.; Stein, O.; Thépaut, J.-N.; Thouret, V.; Vrekoussis, M.; Zerefos, C.; the MACC team. The MACC reanalysis: an 8 yr data set of atmospheric composition, *Atmos. Chem. Phys*. **2013**, 13, 4073-4109.
20. ETC-LC Corine land cover (CLC2006), raster database (version 12/2013). http://www.eea.europa.eu/data-and-maps/data/corine-land-cover-2006-raster-3 (accessed (accessed September 16, 2014)
21. ETC-LC Corine land cover (CLC2000), raster database (version 12/2009). http://www.eea.europa.eu/data-and-maps/data/corine-land-cover-2000-clc2000-100-m-version-12-2009 (accessed October 30, 2013).
22. CGIAR-CSI SRTM 90m Digital Elevation Data. http://srtm.csi.cgiar.org/ (accessed October 30, 2013).
23. Eeftens, M.; Beelen, R.; de Hoogh, K.; Bellander, T.; Cesaroni, G.; Cirach, M.; Declercq, C.; Dėdelė, A.; Dons, E.; de Nazelle, A.; Dimakopoulou, K.; Eriksen, K.; Falq, G.; Fischer, P.; Galassi, C.; Gražulevičienė, R.; Heinrich, J.; Hoffmann, B.; Jerrett, M.; Keidel, D.; Korek, M.; Lanki, T.; Lindley, S.; Madsen, C.; Mölter, A.; Nádor, G.; Nieuwenhuijsen, M.; Nonnemacher, M.; Pedeli, X.; Raaschou-Nielsen, O.; Patelarou, E.; Quass, U.; Ranzi, A.; Schindler, C.; Stempfelet, M.; Stephanou, E.; Sugiri, D.; Tsai, M.-Y.; Yli-Tuomi, T.; Varró, M. J.; Vienneau, D.; Klot, S. v.; Wolf, K.; Brunekreef, B.; Hoek, G. Development of land use regression models for PM2.5, PM2.5 absorbance, PM10 and PMcoarse in 20 European study areas; Results of the ESCAPE Project. *Environ. Sci. Technol.* **2012b**, 46 (20), 11195−11205.
24. Giordano, L.; Brunner, D.; Flemming, J.; Hogrefe, C.; Im, U.; Bianconi, R.; Badia, A.; Balzarini, A.; Baró, R.; Chemel, C.; Curci, G.; Forkel, R.; Jiménez-Guerrero, P.; Hirtl, M.; Hodzic, A.; Honzak, L.; Jorba, O.; Knote, C.; Kuenen, J. J. P.; Makar, P. A.; Manders-Groot, A.; Neal, L.; Pérez, J. L.; Pirovano, G.; Pouliot, G.; San José, R.; Savage, N.; Schröder, W.; Sokhi, R. S.; Syrakov, D.; Torian, A.; Tuccella, P.; Werhahn, J.; Wolke, R.; Yahya, K.; Žabkar, R.; Zhang, Y.; Galmarini, S. Assessment

of the MACC reanalysis and its influence as chemical boundary conditions for regional air quality modeling in AQMEII-2. *Atmos. Environ.* **2015**, 115, 371-388.
25. Kharol, S. K.; Martin, R.V.; Philip, S.; Boys, B.; Lamsal, L. N.; Jerrett, M.; Brauer, M.; Crouse, D. L.; McLinden, C.; Burnett, R. T.; Assessment of the Magnitude and Recent Trends in Satellite-Derived Ground-Level Nitrogen Dioxide over North America, *Atmos. Environ*. **2015**, 118, 236–245.
26. Hystad, P.; Demers, P.; Johnson, K.; Brook, J.; van Donkelaar, A.; Lamsal, L.; Martin, R.; Brauer, M. Spatiotemporal air pollution exposure assessment for a Canadian population-based lung cancer case-control study. *Environ. Health* **2012**, 11 (1), 22
27. Wang, M.; Beelen, R.; Bellander, T.; Birk, M.; Cesaroni, G.; Cirach, M.; Cyrys, J.; de Hoogh, K.; Declercq, C.; Dimakopoulou, K.; Eeftens, M.; Eriksen, K. T.; Forastiere, F.; Galassi, C.; Grivas, G.; Heinrich, J.; Hoffmann, B.; Ineichen, A.; Korek, M.; Lanki, T.; Lindley, S.; Modig, L.; Molter, A.; Nafstad, P.; Nieuwenhuijsen, M. J.; Nystad, W.; Olsson, D.; Raaschou-Nielsen, O.; Ragettli, M.; Ranzi, A.; Stempfelet, M.; Sugiri, D.; Tsai, M. Y.; Udvardy, O.; Varro, M.J.; Vienneau, D.; Weinmayr, G.; Wolf, K.; Yli-Tuomi, T.; Hoek, G.; Brunekreef, B. Performance of multi-cities land use regression models for nitrogen dioxide and fine particles. *Environ. Health Perspect.* **2014**, 122, 843-849.

List of Tables and Figures

Table 1: Descriptive statistics for monitoring data

	Site type	N	Mean[1]	Median[1]	SD[1]	P05[1]	P25[1]	P75[1]	P95[1]	Kurtosis	Skewness
$PM_{2.5}$											
ESCAPE	Rural BG[2]	54	13.7	13.9	4.7	5.3	9.4	16.8	21.8	-0.51	-0.05
	Street	207	17.2	17.1	5.9	8.9	12.3	20.5	29.8	0.41	0.68
	Urban BG[2]	175	15.0	14.8	5.3	7.5	11.0	18.5	24.7	0.04	0.50
	Total	436	15.9	15.8	5.7	7.9	11.7	19.2	25.9	0.46	0.61
AIRBASE	BG[2]	345	15.8	15.8	5.2	7.3	12.7	18.9	23.7	0.60	0.22
	Industrial	53	15.1	15.3	5.5	7.7	10.4	18.8	25.6	-0.79	0.41
	Traffic	151	16.3	16.6	4.9	8.5	13.0	19.7	23.7	-0.61	0.01
	Total	549	15.9	15.9	5.1	7.7	12.5	19.3	23.9	0.11	0.18
NO_2											
ESCAPE	Rural BG[2]	119	14.4	14.8	6.3	2.3	9.5	18.0	26.2	-0.10	0.20
	Street	739	38.1	33.4	18.0	16.2	25.3	48.6	72.8	1.15	1.08
	Urban BG[2]	578	23.2	22.3	10.5	7.8	14.8	29.9	42.8	-0.01	0.54
	Total	1436	30.1	26.8	16.9	9.5	18.0	37.7	64.7	2.15	1.28
AIRBASE	BG[2]	1288	21.5	21.0	9.8	5.7	14.8	28.0	37.2	0.19	0.35
	Industrial	372	19.4	18.2	10.1	4.5	11.5	26.7	38.1	0.14	0.61
	Traffic	740	40.2	38.7	14.6	20.3	30.4	47.7	65.8	1.92	0.92
	Total	2400	26.9	25.1	14.6	6.8	16.4	34.7	53.7	1.98	1.02

1) in $\mu g/m^3$
2) BG = Background

Table 2: Comparison of basic performance statistics (R^2, SEE) for all models including derivation, HOV, COV and COHOV

	Model[a]	Predictor variables[b]	DERIVATION[c] R^2	DERIVATION[c] Adj R^2	DERIVATION[c] SEE[g]	HOV[d] R^2	HOV[d] SEE[g]	COV[e] R^2	COV[e] SEE[g]	COHOV[f] R^2	COHOV[f] SEE[g]
$PM_{2.5}$											
ESCAPE	M1	All roads (0.7km), Urban green (1.8km), Natural (10km), Residential, Major roads (0.1km), Y coordinate	0.394	0.383	4.43	0.318	4.77	0.205	4.57	0.220	4.78
	M2	PM2.5 SAT, All roads (5km), Residential, Altitude, Major roads, Y coordinate	0.591	0.584	3.65	0.510	4.03	0.575	3.35	0.553	3.61
	M3	PM2.5 CTM, All roads (0.1km), Natural (0.8km), Residential, Major roads, Y coordinate	0.410	0.400	4.37	0.369	4.59	0.282	4.34	0.293	4.55
	M4	PM2.5 SAT, PM2.5 CTM, All roads (0.7km), Residential, Major roads, Altitude, Y coordinate	0.606	0.598	3.59	0.544	3.89	0.592	3.30	0.485	4.01
AIRBASE	M1	Natural (10km), Natural (0.4km), Urban green (10km), Altitude, Major roads (0.1km), Residential, Urban green (0.6km), Ind/comm(10km), Y coordinate	0.339	0.325	4.15	0.268	4.63	0.388	4.43	0.412	4.43
	M2	PM2.5 SAT, Altitude, Natural (0.2km), All roads (0.1km), Residential (0.2km), Major roads, Y coordinate	0.613	0.606	3.18	0.562	3.58	0.558	3.77	0.510	4.03
	M3	PM2.5 CTM, Altitude, Residential (0.2km), Major roads (0.1km), Natural (0.1km), Urban green (1.8km)	0.527	0.520	3.50	0.445	4.03	0.230	4.97	0.295	4.85
	M4	PM2.5 SAT, PM2.5 CTM, Altitude, Residential (0.2km), Major roads (0.1km), Natural (0.1km), Y coordinate	0.636	0.630	3.08	0.583	3.49	0.523	3.91	0.534	3.93
NO_2											
ESCAPE	M1	All roads (5km), All roads (0.2km), Residential (1.8km), Major roads, Ind/comm(10km), Ports (0.4km), Y coordinate	0.474	0.471	12.10	0.377	14.22	0.463	10.69	0.490	10.63
	M2	NO2 SAT, All roads (5km), All roads (0.2km), Urban green (1.8km), Residential (1.5km), Major roads, Ind/comm(10km), Ports (0.4km), Y coordinate	0.514	0.510	11.64	0.400	13.95	0.505	10.26	0.516	10.36
	M3	NO2 CTM, Major roads, Residential (1.5km), All roads (0.2km), All roads (2km), Urban green, Y coordinate	0.573	0.571	10.90	0.442	13.45	0.553	9.75	0.563	9.84
	M4	n.a.									
AIRBASE	M1	All roads (2km), Major roads (0.1km), Total build up (10km), Natural (1.5km), Residential (0.5km), Ports (0.2km), Altitude, All roads, Y coordinate	0.516	0.513	10.13	0.536	10.14	0.366	13.46	0.295	15.13
	M2	NO2 SAT, Major roads (0.1km), All roads (10km), Residential (1.8km), Ports (0.2km), Residential (0.3km), All roads (10km), Y coordinate	0.537	0.535	9.90	0.549	10.00	0.416	12.92	0.350	14.53
	M3	NO2 CTM, Major roads (0.1km), All roads (2km), All roads, Ports (0.2km), Residential (0.3km), Natural (0.5km)	0.582	0.581	9.40	0.599	9.43	0.502	11.93	0.425	13.66
	M4	n.a.									

a) M1= no SAT or CTM; M2= including SAT; M3= including CTM; M4 = including both SAT and CTM

b) Predictor variables without a distance attached are the origin cell without a focalsum (e.g. for CORINE variables this is the value within the 100x100m cell).

c) Derivation: model development on 80% of monitoring sites

d) HOV: hold-out-validation on 20% of monitoring sites

e) COV: cross-over-validation on full dataset (COV for ESCAPE model on AIRBASE full monitoring sites and vice versa)

f) COHOV: cross-over-hold-out-validation on 20% of the dataset (COHOV for ESCAPE model on the HOV dataset from AIRBASE monitoring sites and vice versa)

g) Standard Error Estimate ($\mu g/m^3$)

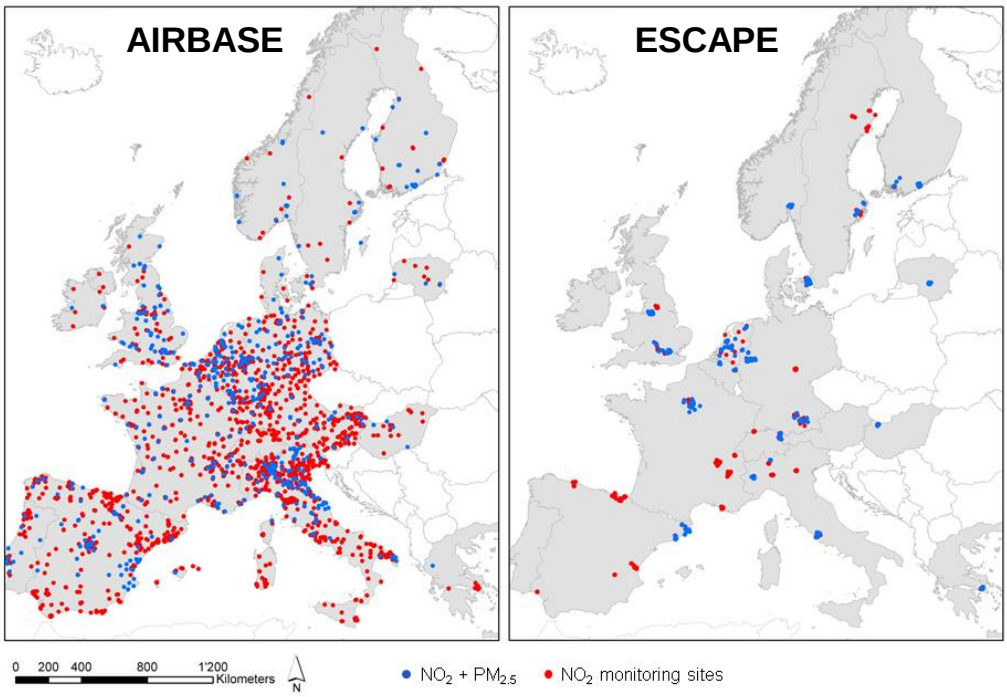

Figure 1: Location of AIRBASE and ESCAPE monitoring sites for $PM_{2.5}$ and NO_2

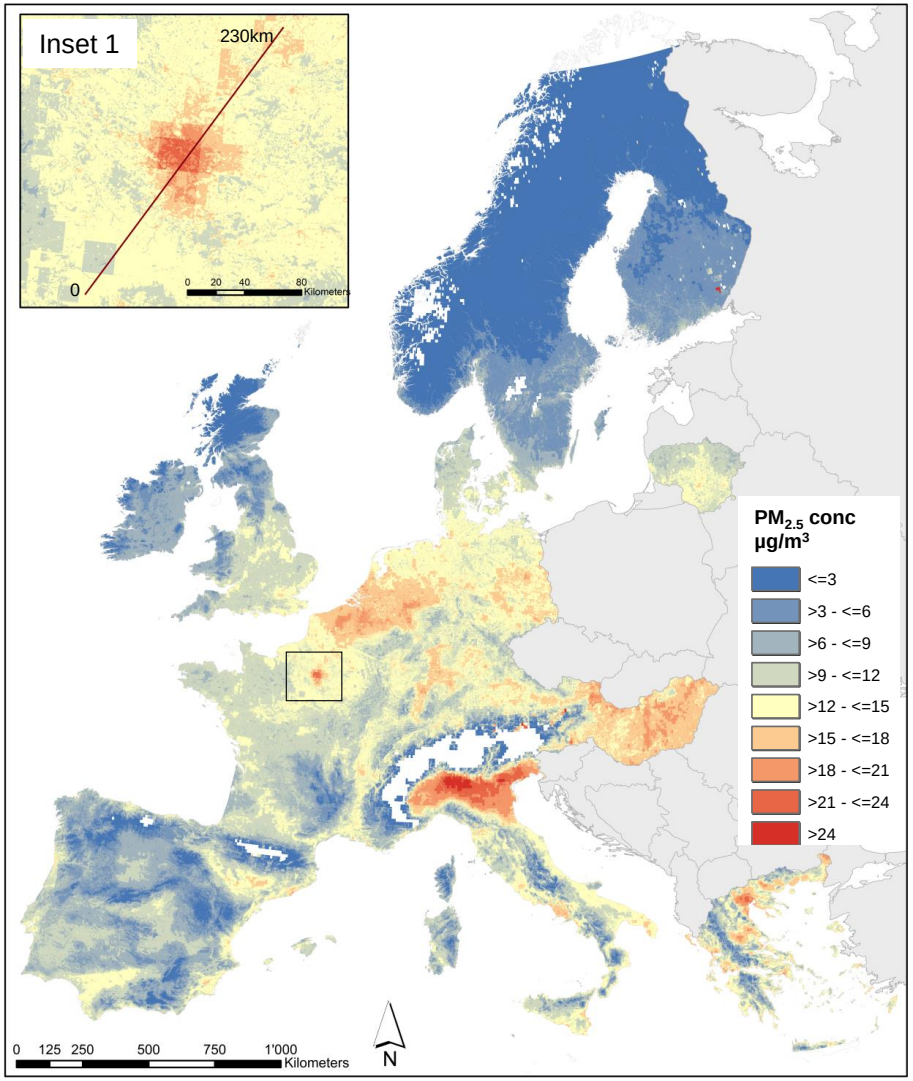

Model 4 AIRBASE $PM_{2.5}$

Transect (red line in Inset 1) through Paris and surrounding area (0-230km) showing the contribution of each predictor variable of Model 4 (in µg/m³) and the final modelled $PM_{2.5}$ concentration in red.

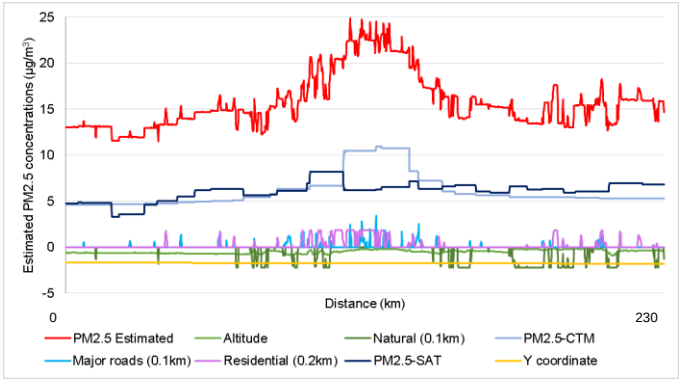

Scatterplots showing measured versus predicted $PM_{2.5}$ concentrations at both the HOV and the COV validation data sets

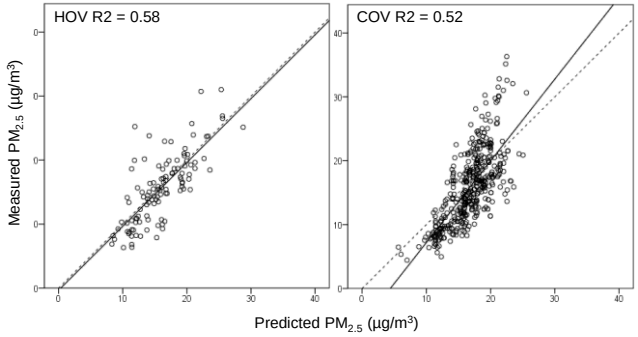

Figure 2: Map and profile plot of $PM_{2.5}$ concentration predicted by Model 4 (with SAT and CTM) using AIRBASE sites in 2010; scatterplots of modelled vs. measured $PM_{2.5}$ at evaluation sites

Supplemental Information

Table S1: Descriptive statistics monitoring data by region (in µg/m^3)

Pollutant	Network	Region[1]	Mean	Min	P05	P95	Max	SD	Count
$PM_{2.5}$	ESCAPE	N	11.7	4.4	6.4	21.8	30.3	5.4	99
		W	15.2	7.0	8.9	21.1	30.6	4.2	119
		C	16.8	8.8	11.7	23.3	26.2	4.1	78
		S	18.9	8.4	11.3	30.6	36.3	5.7	140
	AIRBASE	N	10.2	2.1	4.9	17.8	20.1	3.4	59
		W	16.2	4.3	9.8	22.0	26.0	3.7	185
		C	18.0	6.3	13.0	23.0	27.3	3.4	129
		S	15.9	3.6	6.7	28.1	33.4	6.4	176
NO_2	ESCAPE	N	17.1	1.5	5.6	34.6	59.8	9.5	240
		W	30.5	6.9	13.6	56.7	102.7	14.1	319
		C	27.8	5.5	12.3	50.9	88.0	11.9	343
		SW	37.7	1.9	11.6	76.4	109.0	20.9	314
		SE	36.8	5.3	11.0	67.7	100.2	17.9	220
	AIRBASE	N	23.8	0.4	1.3	47.0	61.0	14.8	101
		W	27.4	3.0	10.6	51.5	98.3	13.5	665
		C	28.1	2.6	8.5	56.6	99.9	15.3	626
		SW	21.4	1.5	3.7	46.6	67.9	13.4	438
		SE	30.0	1.3	8.5	58.5	101.8	14.7	570

1) N = North, W = West, C = Central, S = South, SW = South West, SE = South East

Table S2: GIS predictor variables

Data set	Predictor variable[a]	Name variable	Buffer Size (radius in m) or point estimate
$PM_{2.5}$ ($\mu g/m^3$) derived from the MODIS, MISR, and SeaWiFS satellite instruments	Surface $PM_{2.5}$ concentration derived from satellite	SAT-PM_{25}	Point (~10km spacing)
NO_2 ($\mu g/m^3$) derived from OMI on board the Aura satellite	Surface NO_2 concentration derived from satellite	SAT-NO_2	Point (~10km spacing)
$PM_{2.5}$ and NO_2 ($\mu g/m^3$) estimated by MACC-II Ensemble model	Surface $PM_{2.5}$ and NO_2 concentration from dispersion model	CTM-PM_{25} CTM-NO_2	Point (~10km spacing)
EuroStreets roads (length in m)	Major roads All roads	Major roads All roads	50; 100; 200; 300; 400; 500; 700; 1000; 2000; 5000; 10000
Corine land cover	Industry/commercial Ports Urban green Total built up[b] Natural land Residential[c]	Ind/comm Ports Urban green Total build up Natural Residential	50; 100; 200; 300; 400; 500; 600; 700; 800; 1000; 1200; 1500; 1800; 2000; 2500; 3000; 3500; 4000; 5000; 6000; 7000; 8000; 10000
Altitude 90 m SRTM DTM Trend	Altitude – transformed[d] North-South trend	Altitude Ycoord	Point Point

[a]Prespecified direction of effect is negative for: Urban green, Natural and Altitude [b]Residential + Ind/comm + Port + transport infrastructure, airports, mines, dumps and construction sites [c]continuous urban fabric (high density housing) + discontinuous urban fabric (low density housing) [d]Transformed altitude is calculated as $\sqrt{(nalt/max(nalt))}$, where nalt = altitude − min(altitude).

Table S3: Model variables and derivation statistics

	ESCAPE					AIRBASE				
	Variables	ß[a]	VIF	R^{2b}	P95-P5[c]	Variables	ß[a]	VIF	R^{2b}	P95-P5[c]
$PM_{2.5}$										
M1	Constant	26.18				Constant	22.48			
	All roads (0.7km)	1.34E-04	1.315	0.065	1.62	Natural (10km)	-1.65E-04	1.632	0.164	-3.61
	Urban green (1.8km)	-5.85E-03	1.144	0.071	-1.20	Natural (0.4km)	-6.22E-02	1.399	0.204	-1.69
	Natural (10km)	-2.70E-04	1.080	0.158	-6.42	Urban green (10km)	-8.64E-04	1.855	0.224	-3.09
	Residential	1.91E+00	1.086	0.172	1.91	Altitude	-5.53E-03	1.517	0.239	-3.50
	Major roads (0.1km)	5.19E-03	1.145	0.179	2.20	Major roads (0.1km)	3.24E-03	1.061	0.254	1.71
	Y coordinate	-3.58E-06	1.146	0.383	-8.62	Residential	1.30E+00	1.295	0.268	1.30
						Urban green (0.6km)	-3.39E-02	1.155	0.271	-0.85
						Ind/comm(10km)	8.44E-04	1.649	0.291	2.70
						Y coordinate	-1.85E-06	1.446	0.325	-4.01
M2	Constant	8.04				Constant	10.75			
	PM2.5 SAT	7.85E-01	1.224	0.449	10.99	PM2.5 SAT	5.95E-01	1.114	0.480	10.18
	All roads (5km)	6.70E-06	1.170	0.508	2.42	Altitude	-5.42E-03	1.339	0.533	-3.44
	Residential	1.79E+00	1.044	0.521	1.79	Natural (0.2km)	-1.96E-01	1.291	0.559	-1.57
	Altitude	-4.65E-03	1.141	0.525	-2.23	All roads (0.1km)	1.55E-03	1.526	0.577	1.27
	Major roads	1.30E-02	1.049	0.530	1.56	Residential (0.2km)	1.39E-01	1.322	0.589	1.80
	Y coordinate	-1.94E-06	1.271	0.584	-4.67	Major roads	5.31E-03	1.392	0.590	1.05
						Y coordinate	-1.23E-06	1.341	0.606	-2.67
M3	Constant	21.06				Constant	3.81			
	PM2.5 CTM	2.93E-01	1.439	0.201	3.29	PM2.5 CTM	1.06E+00	1.026	0.406	10.49
	All roads (0.1km)	1.68E-03	1.385	0.231	1.40	Altitude	-4.36E-03	1.091	0.460	-2.76
	Natural (0.8km)	-3.44E-04	1.189	0.246	-4.85	Residential (0.2km)	1.19E-01	1.202	0.490	1.55
	Residential	1.80E+00	1.041	0.261	1.80	Major roads (0.1km)	3.23E-03	1.026	0.501	1.71
	Major roads	1.36E-02	1.355	0.265	1.63	Natural (0.1km)	-6.22E-01	1.247	0.512	-1.87
	Y coordinate	-3.19E-06	1.369	0.400	-7.68	Urban green (1.8km)	-6.65E-03	1.030	0.520	-1.09
M4	Constant	4.92				Constant	5.96			
	PM2.5 SAT	7.48E-01	1.289	0.449	10.47	PM2.5 SAT	4.39E-01	2.071	0.480	7.50
	PM2.5 CTM	2.38E-01	1.339	0.512	2.67	PM2.5 CTM	4.55E-01	2.383	0.527	4.51
	All roads (0.7km)	1.72E-04	1.317	0.556	2.08	Altitude	-4.83E-03	1.353	0.579	-3.06
	Residential	1.64E+00	1.090	0.564	1.64	Residential (0.2km)	1.40E-01	1.231	0.611	1.82
	Major roads	1.14E-02	1.104	0.567	1.37	Major roads (0.1km)	2.90E-03	1.030	0.621	1.53
	Altitude	-4.12E-03	1.150	0.571	-1.98	Natural (0.1km)	-4.50E-01	1.255	0.627	-1.35
	Y coordinate	-1.51E-06	1.481	0.598	-3.63	Y coordinate	-6.00E-07	1.539	0.630	-1.30
NO_2[d]										
M1	Constant	23.59				Constant	16.83			
	All roads (5km)	4.25E-05	2.860	0.342	14.79	All roads (2km)	1.24E-04	2.542	0.356	8.79
	All roads (0.2km)	4.75E-03	1.352	0.380	7.55	Major roads (0.1km)	1.59E-02	1.496	0.422	7.61
	Residential (1.8km)	1.33E-02	1.790	0.390	10.94	Total build up (10km)	6.38E-04	1.927	0.457	12.43
	Major roads	3.87E-02	1.217	0.398	5.61	Natural (1.5km)	-6.30E-03	1.654	0.472	-3.12
	Ind/comm (10km)	1.69E-03	1.725	0.400	5.66	Residential (0.5km)	9.39E-02	1.640	0.494	7.60
	Ports (0.4km)	5.25E-01	1.033	0.401	0.00	Ports (0.2km)	1.03E+00	1.033	0.499	0.00
	Y coordinate	-6.22E-06	1.089	0.471	-15.22	Altitude	-2.73E-03	1.291	0.500	-1.90
						All roads	2.11E-02	1.553	0.510	5.07
						Y coordinate	-1.60E-06	1.127	0.513	-2.85
M2	Constant	21.99				Constant	13.67			
	NO2 SAT	1.13E+00	1.160	0.116	11.33	NO2 SAT	1.03E+00	1.403	0.127	9.48
	All roads (5km)	3.72E-05	2.870	0.367	12.93	Major roads (0.1km)	1.60E-02	1.496	0.263	7.66
	All roads (0.2km)	4.85E-03	1.357	0.406	7.71	All roads (10km)	1.17E-05	1.802	0.409	10.86
	Urban green (1.8km)	-1.35E-02	1.231	0.427	-2.57	Residential (1.8km)	1.17E-02	2.900	0.492	9.99
	Residential (1.5km)	1.65E-02	1.656	0.436	9.58	Ports (0.2km)	1.21E+00	1.017	0.497	0.00
	Major roads	3.77E-02	1.218	0.445	5.47	Residential (0.3km)	2.00E-01	2.159	0.512	5.81
	Ind/comm(10km)	1.52E-03	1.721	0.446	5.10	All roads (10km)	2.35E-02	1.524	0.526	5.66
	Ports (0.4km)	5.98E-01	1.035	0.448	0.00	Y coordinate	-2.68E-06	1.169	0.535	-4.77
	Y coordinate	-6.40E-06	1.296	0.514	-15.66					
M3	Constant	12.38				Constant	3.59			
	NO2 CTM	9.50E-01	1.216	0.371	24.83	NO2 CTM	8.12E-01	1.189	0.288	17.25
	Major roads	4.55E-02	1.193	0.414	6.60	Major roads (0.1km)	1.52E-02	1.480	0.405	7.27
	Residential (1.5km)	1.12E-02	1.724	0.471	6.50	All roads (2km)	1.69E-04	1.670	0.533	11.95
	All roads (0.2km)	4.55E-03	1.424	0.506	7.24	All roads	2.19E-02	1.551	0.548	5.26
	All roads (2km)	1.31E-04	2.023	0.534	9.40	Ports (0.2km)	9.27E-01	1.020	0.549	0.00
	Urban green	-6.28E+00	1.004	0.536	0.00	Residential (0.3km)	2.26E-01	1.537	0.579	6.54
	Y coordinate	-4.44E-06	1.116	0.571	-10.86	Natural (0.5km)	-4.59E-02	1.368	0.581	-2.43

a) All p-values < 0.05

b) Incremental partial R^2

c) Regression slope (ß) in $\mu g/m^3$ were multiplied by the difference between the 5th and 95th percentile of each predictor. The value shown in the P95 – P5.

d) No valid models were possible for NO_2 M4

Table S4: Performance indicators for HOV; slope and constant for HOV, COV and COHOV validation sets

	HOV performance indicators					HOV		COV		COHOV	
Model	ME[a]	AE[b]	MB[c]	AB[d]	FB[e]	β	Constant	β	Constant	β	Constant
PM2.5 ESCAPE											
M1	-0.08	3.62	7.71	24.73	-0.005	0.96	0.78	0.65	5.82	0.67	5.58
M2	0.21	3.25	6.94	21.45	0.018	0.99	0.01	0.77	4.31	0.77	4.13
M3	0.00	3.48	7.26	23.26	0.000	0.96	0.62	0.77	4.28	0.74	4.69
M4	0.27	3.13	6.81	20.48	0.022	1.00	-0.26	0.76	4.34	0.74	5.13
PM2.5 AIRBASE											
M1	0.03	3.64	9.85	27.23	0.002	0.97	0.38	1.36	-6.33	1.48	-8.35
M2	0.37	2.66	8.86	20.03	0.023	1.02	-0.66	1.38	-6.99	1.32	-6.40
M3	0.52	3.12	10.58	22.79	0.032	0.93	0.59	0.67	4.32	0.76	2.65
M4	0.37	2.57	8.29	18.84	0.023	1.00	-0.34	1.28	-5.63	1.31	-6.58
NO2 ESCAPE											
M1	-0.88	9.75	13.10	36.19	-0.029	0.96	2.07	0.90	4.50	0.95	3.34
M2	-1.09	9.44	10.59	34.93	-0.036	0.98	1.79	0.94	3.13	0.95	2.75
M3	-0.86	9.07	9.32	33.95	-0.029	0.96	2.09	0.97	2.64	0.97	2.45
NO2 AIRBASE											
M1	-0.15	7.47	21.49	40.21	-0.006	1.08	-1.90	1.14	-6.80	1.09	-4.01
M2	-0.05	7.25	19.80	37.70	-0.002	1.02	-0.59	1.09	-4.83	1.10	-3.85
M3	0.00	6.53	14.49	30.17	0.000	1.03	-0.77	1.15	-7.04	1.15	-5.99

a) mean error ($\mu g/m^3$)
b) absolute error ($\mu g/m^3$)
c) mean bias ($\mu g/m^3$)
d) absolute bias ($\mu g/m^3$)
e) fractional bias

Table S5: Regional validation (HOV and COV) of all models

Model	Region[a]	HOV R^2	HOV RMSE[b]	HOV N[c]	COV R^2	COV RMSE[b]	COV N[c]	HOV R^2	HOV RMSE[b]	HOV N[c]	COV R^2	COV RMSE[b]	COV N[c]
		$PM_{2.5}$ ESCAPE						$PM_{2.5}$ AIRBASE					
M1	N	0.230	4.62	21	0.271	2.93	59	0.087	2.1	16	0.445	4.04	99
	W	0.167	3.55	27	0.176	3.36	185	0.148	3.49	35	0.523	2.87	119
	C	0.320	4.22	14	0.196	3.05	129	0.652	2.2	21	0.508	2.9	78
	S	0.272	5.9	27	0.046	6.28	176	0.135	6	40	0.064	5.58	140
M2	N	0.528	3.69	21	0.334	2.8	59	0.094	2.09	16	0.616	3.36	99
	W	0.497	2.76	27	0.374	2.93	185	0.275	3.13	35	0.613	2.6	119
	C	0.195	4.24	14	0.324	2.8	129	0.655	2.23	21	0.226	3.55	78
	S	0.491	4.93	27	0.606	4.06	176	0.512	4.51	40	0.508	4.04	140
M3	N	0.314	4.45	21	0.329	2.82	59	0.41	1.69	16	0.48	3.91	99
	W	0.372	3.08	27	0.344	3	185	0.264	3.24	35	0.463	3.06	119
	C	0.384	4.02	14	0.244	2.96	129	0.745	1.88	21	0.471	3.01	78
	S	0.346	5.59	27	0.101	6.1	176	0.39	5.04	40	0.037	5.75	140
M4	N	0.556	3.58	21	0.345	2.78	59	0.187	1.98	16	0.654	3.19	99
	W	0.585	2.51	27	0.385	2.91	185	0.305	3.15	35	0.645	2.49	119
	C	0.316	3.91	14	0.336	2.77	129	0.724	1.96	21	0.303	3.37	78
	S	0.577	4.5	27	0.631	3.93	176	0.528	4.43	40	0.444	4.3	140
		NO_2 ESCAPE						NO_2 AIRBASE					
M1	N	0.388	7.46	40	0.450	11.01	101	0.599	9.1	19	0.356	7.65	240
	W	0.364	10.96	51	0.473	9.82	665	0.455	9.43	120	0.602	8.87	319
	C	0.491	9.23	69	0.574	9.97	626	0.572	10.72	122	0.458	8.73	343
	SW	0.291	19.69	66	0.659	7.81	438	0.686	7.83	102	0.354	16.84	314
	SE	0.345	15.43	51	0.398	11.41	570	0.523	10.14	113	0.313	14.82	220
M2	N	0.376	7.53	40	0.419	11.32	101	0.562	9.53	19	0.337	7.75	240
	W	0.412	10.54	51	0.546	9.11	665	0.447	9.49	120	0.593	8.97	319
	C	0.516	9.00	69	0.575	9.96	626	0.546	11.05	122	0.455	8.76	343
	SW	0.312	19.40	66	0.685	7.50	438	0.680	7.91	102	0.386	16.42	314
	SE	0.463	13.97	51	0.431	11.09	570	0.556	9.79	113	0.494	12.74	220
M3	N	0.498	6.75	40	0.456	10.89	101	0.590	9.22	19	0.408	7.34	240
	W	0.454	10.15	51	0.573	8.83	665	0.485	9.17	120	0.629	8.57	319
	C	0.452	9.58	69	0.598	9.69	626	0.565	10.82	122	0.470	8.64	343
	SW	0.324	19.24	66	0.721	7.07	438	0.770	6.70	102	0.462	15.36	314
	SE	0.530	13.07	51	0.499	10.41	570	0.607	9.21	113	0.534	12.22	220

a) N = North; W = West; C = Central; S = South; SW = South West; SE = South East

b) Rout Mean Square Error ($\mu g/m^3$)

c) Number of sites

Table S6: Performance of models (R^2, RSME) by site type

	HOV						COV					
Model	R^2	RSME	R^2	RSME	R^2	RSME	R^2	RSME	R^2	RSME	R^2	RSME
$PM_{2.5}$ ESCAPE	Urban BG (n = 31)		Street (n = 44)		Rural BG (n = 14)		Background (n = 345)		Traffic (n = 151)		Industrial (n = 53)	
M1	0.19	3.56	0.40	4.94	0.09	4.77	0.22	4.56	0.26	4.23	0.02	5.45
M2	0.43	2.97	0.51	4.49	0.50	3.54	0.64	3.12	0.52	3.44	0.39	4.30
M3	0.24	3.44	0.41	4.90	0.15	4.59	0.31	4.30	0.32	4.07	0.09	5.27
M4	0.49	2.83	0.53	4.38	0.48	3.59	0.65	3.05	0.52	3.42	0.44	4.12
$PM_{2.5}$ AIRBASE	Background (n = 70)		Traffic (n = 30)		Industrial (n = 12)		Urban BG (n = 175)		Street (n = 207)		Rural BG (n = 54)	
M1	0.34	4.35	0.25	4.41	0.29	5.56	0.31	4.43	0.42	4.47	0.38	3.70
M2	0.67	3.10	0.53	3.48	0.12	6.19	0.59	3.42	0.49	4.21	0.69	2.60
M3	0.53	3.66	0.32	4.20	0.27	5.66	0.15	4.93	0.25	5.08	0.41	3.59
M4	0.68	3.02	0.52	3.52	0.18	5.99	0.49	3.81	0.51	4.12	0.66	2.72
NO_2 ESCAPE	Urban BG (n = 111)		Street (n = 144)		Rural BG (n = 22)		Background (n = 1288)		Traffic (n = 740)		Industrial (n = 372)	
M1	0.46	7.47	0.34	16.20	0.34	4.02	0.47	7.16	0.24	12.72	0.41	7.81
M2	0.53	7.02	0.36	15.87	0.60	3.13	0.58	6.38	0.28	12.46	0.56	6.73
M3	0.62	6.29	0.42	15.14	0.50	3.52	0.67	5.64	0.30	12.25	0.61	6.36
NO_2 AIRBASE	Background (n = 262)		Traffic (n = 132)		Industrial (n = 80)		Urban BG (n = 578)		Street (n = 739)		Rural BG (n = 119)	
M1	0.54	6.86	0.31	12.52	0.52	7.03	0.42	4.97	0.24	15.70	0.37	5.02
M2	0.60	6.41	0.31	12.46	0.61	6.27	0.51	7.34	0.30	15.03	0.56	4.19
M3	0.72	5.34	0.32	12.40	0.72	5.34	0.62	6.44	0.40	13.93	0.59	4.09

Table S7: Combined models using AIRBASE and ESCAPE sites (coefficients, partial R^2, VIF, SEE, HOV R^2 and SEE)

		DERIVATION				HOV	
Pollutant	Variables	ß[a]	VIF	R^{2b}	SEE	R^2	SEE
$PM_{2.5}$	Constant	6.778					
	PM2.5 SAT	5.81E-01	1.490	0.457			
	PM2.5 CTM	2.48E-01	2.051	0.504			
	Total build up (0.2km)	1.33E-01	1.680	0.536			
	Altitude	-4.68E-03	1.261	0.548			
	Urban green (10km)	-6.71E-04	2.079	0.565			
	All roads (0.1km)	1.55E-03	1.582	0.582			
	All roads (5km)	4.86E-06	2.686	0.589			
	Natural (0.2km)	-1.52E-01	1.385	0.593			
	Major roads	7.06E-03	1.379	0.596			
	Y coordinate	-9.84E-07	1.752	0.604			
	Network[c]	-6.23E-01	1.139	0.606	3.34	0.588	3.55
NO_2	Constant	7.703					
	NO2 CTM	9.65E-01	1.303	0.330			
	All roads (1km)	4.11E-04	2.044	0.480			
	Major roads (0.1km)	1.42E-02	1.403	0.522			
	Residential (1.5km)	1.38E-02	2.931	0.539			
	All roads	2.18E-02	1.461	0.550			
	Urban green (10km)	-4.86E-04	1.664	0.558			
	Total build up (0.4km)	7.07E-02	2.335	0.560			
	Ports (0.3km)	3.22E-01	1.034	0.561			
	Y coordinate	-2.73E-06	1.359	0.570			
	Network[c]	-2.01E+00	1.148	0.574	10.07	0.533	11.06

a) All p-values < 0.05
b) Incremental partial R^2
c) Network variable coded AIRBASE = 0; ESCAPE = 1.

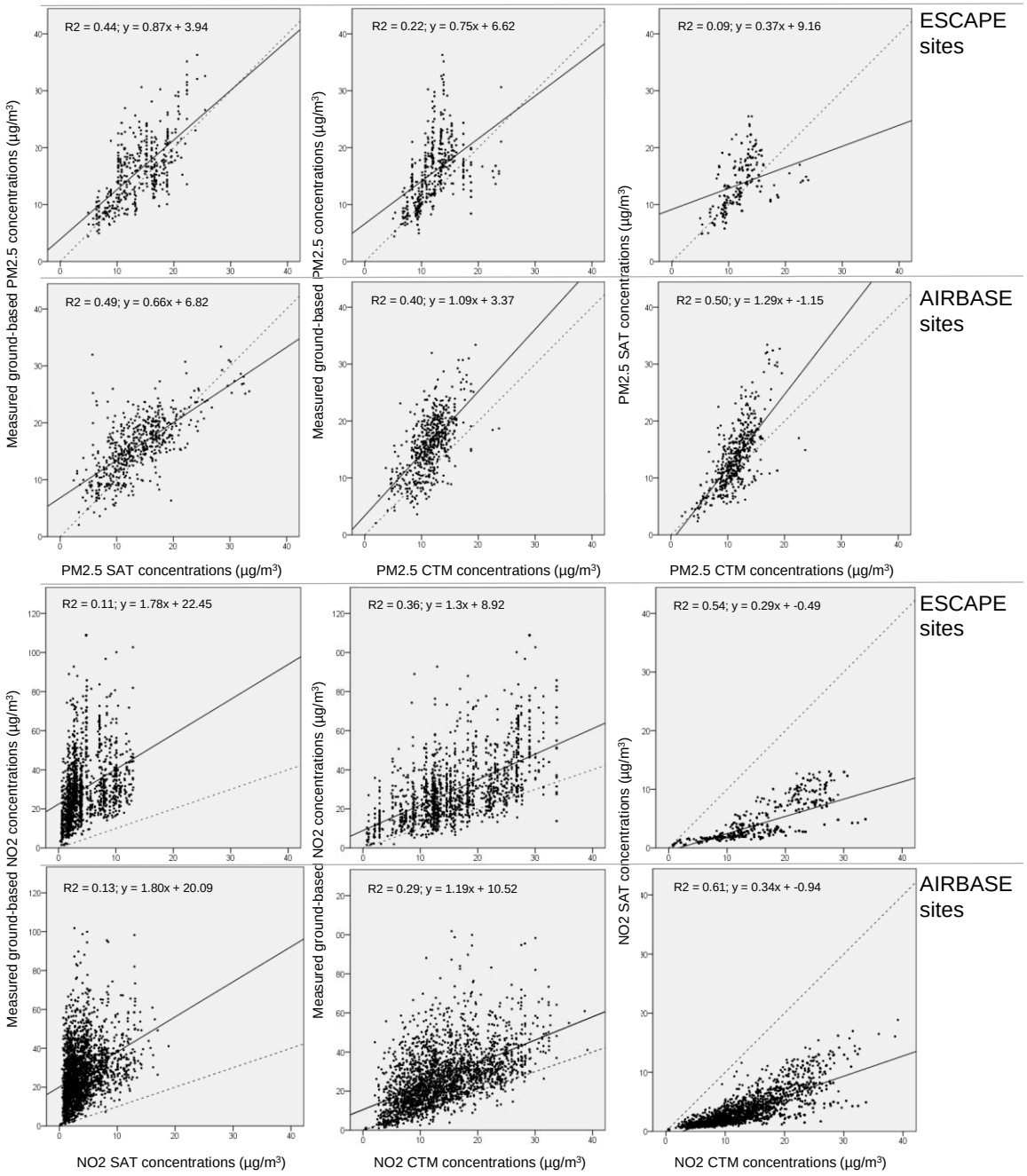

Figure S1: Scatterplots for $PM_{2.5}$ and NO_2 of measured ground based concentrations versus SAT (1st column); versus CTM (2nd column); and SAT versus CTM (3rd column) at ESCAPE and AIRBASE sites. The dotted line denotes the x=y line; the filled line the regression line.

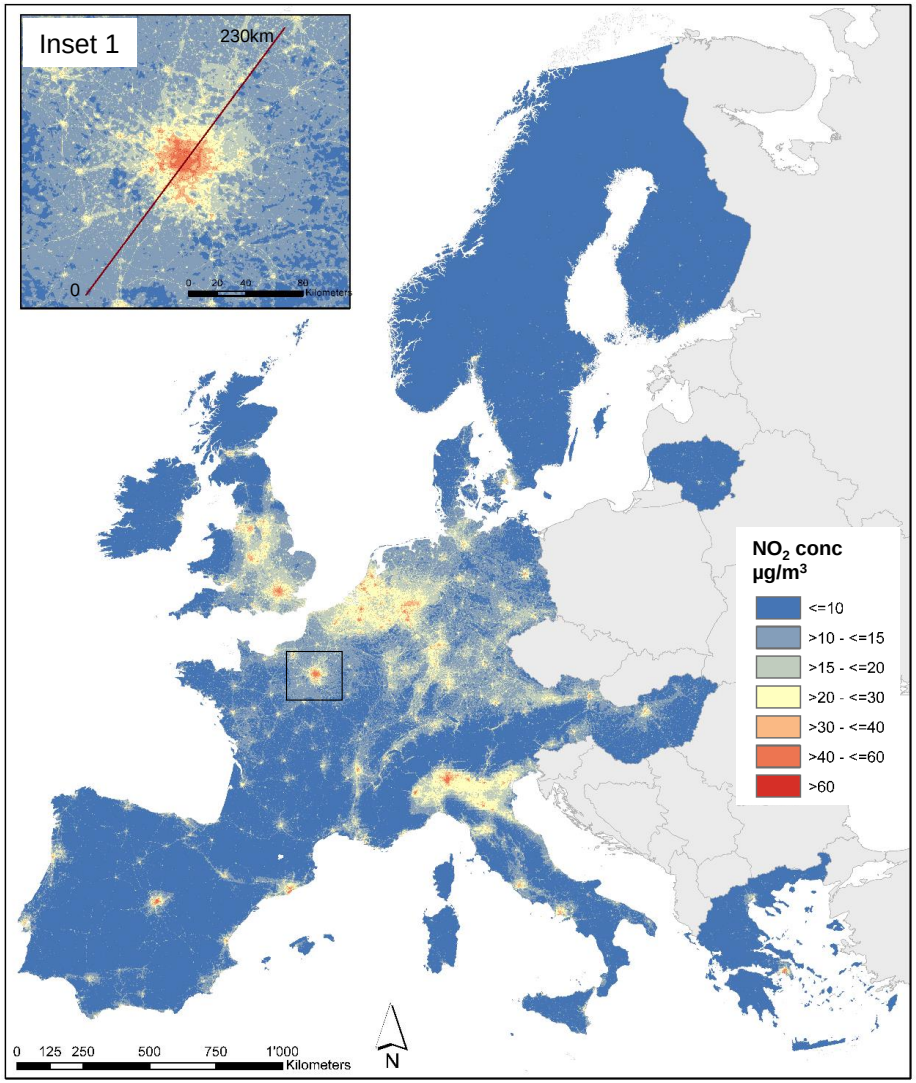

Model 3 AIRBASE NO_2

Transect (red line in Inset 1) through Paris and surrounding area (0-230km) showing the contribution of each predictor variable of Model 2 (in µg/m³) and the final modelled NO_2 concentration in red.

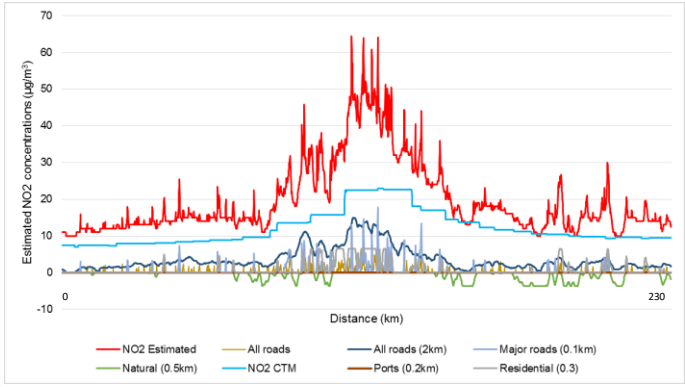

Scatterplots showing measured versus predicted NO_2 concentrations at both the HOV and the COV validation data sets

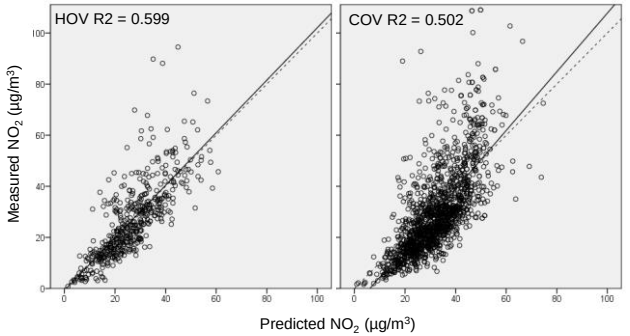

Figure S2: Map and profile plot of NO_2 concentration predicted by Model 3 (with CTM) using AIRBASE sites in 2010; scatterplots of modelled vs. measured NO_2 at evaluation sites